Table 3 *(continued)*

Affymetrix probe set ID	*Gene symbol*	*Gene description*	*Fold change*		
			Dose (mg/kg)		
			15	*50*	*150*
1394068_x_at	Klf2_predicted	Kruppel-like factor 2 (lung) (predicted)	0.74	0.70	0.47
1389681_at	Pvrl2	Poliovirus receptor-related 2	0.88	0.97	0.47
1387307_at	Hal	Histidine ammonia lyase	0.87	0.76	0.47
1373814_at	RGD1310066	Similar to mKIAA1002 protein	0.80	0.84	0.47
1390672_at	Rprm	Candidate mediator of the p53-dependent G2 arrest	0.83	0.79	0.48
1367857_at	Fads1	Fatty acid desaturase 1	1.06	0.93	0.48
1387328_at	Cyp2c	Cytochrome P450, subfamily IIC (mephenytoin 4-hydroxylase)	0.80	1.06	0.48
1386975_at	Pdk2	Pyruvate dehydrogenase kinase, isoenzyme 2	0.61	0.65	0.48
1376785_at	Sycp3	Synaptonemal complex protein 3	0.70	0.85	0.48
1367804_at	Apcs	Serum amyloid P-component	0.70	0.78	0.48
1398759_at	Tgfb1i4	Transforming growth factor beta 1 induced transcript 4	0.72	0.83	0.49
1386041_a_at	Klf2_predicted	Kruppel-like factor 2 (lung) (predicted)	0.83	0.63	0.49
1375599_at	Ddx31_predicted	DEAD/H (Asp-Glu-Ala-Asp/His) box polypeptide 31 (predicted)	0.86	0.57	0.49
1388300_at	Mgst3_predicted	Microsomal glutathione S-transferase 3 (predicted)	0.69	1.00	0.50
1368733_at	Ste	Sulfotransferase, estrogen preferring	0.88	0.98	0.50
1368227_at	Slc28a2	Solute carrier family 28, member 2	1.05	0.84	0.50

Probe sets are sorted by fold change. Shaded probe sets are the ones selected as in-vivo–in-vitro bridging probes (see Figure 3).

sion is similar in rat and human cells but that the extent of the changes is more prominent in rat cells than in human cells. Among them, "protein kinase inhibitor p58", "DnaJ (Hsp40) homolog, subfamily B, member 11", "crystallin, lamda 1", "hypoxia up-regulated 1", and "aldo-keto reductase family 7, member A3 (aflatoxin aldehyde reductase)", which showed remarkable expression changes both in rat *in vivo* and *in vitro*, did not show any significant changes in human hepatocytes. As for the genes such as "ischemia/reperfusion inducible protein", "glutathione reductase", "glutamate-cysteine ligase, catalytic subunit", "NAD(P)H dehydrogenase, quinone 1", and "DNA-damage-inducible transcript 4-like", these were up-regulated in both species, but the extent of up-regulation was much less in human cells than in the rat.

In the next step, changes in expression of these were examined in cells treated with another hepatotoxicant, DFNa, which is known to elicit a similar response as does coumarin, that is, oxidative stress and glutathione depletion.[8,9] Although not all the genes showed changes in common with those observed after coumarin treatment, the trend appeared similar, suggesting that both compounds share the same toxicological pathway(s).

To make a quantitative comparison of responsiveness of the marker genes between species, the mean value of the effect size of the probe sets (TGP2 score) was calculated (Figure 5). It is obvious from the results presented in Figure 5a that the score shows a good dose-dependency, suggesting that the score successfully expresses the responsiveness of cells to the toxicant. Moreover, in the case of coumarin, the score of human hepatocytes to the marker genes is a much lower value than the score observed for rat cells, supporting the known species-specific difference. However, both rat and human cells responded to the markers to the same extent at the same concentration of DFNa. For genes such as "ischemia/reperfusion inducible protein" and "hypoxia up-regulated 1", these were up-regulated in both species at a high-dose DFNa exposure (data not shown). This clearly indicates that the marker genes respond similarly in rat and human hepatocytes when a drug with a similar level of toxicity in each species is applied.

Discussion

Coumarin is a toxin found in many plants, including the tonka bean, and it has clinical value as the precursor for several anticoagulants, especially warfarin. Although coumarin has a sweet scent, its use as a food additive is restricted because of its hepatotoxicity. It is well known that coumarin is a non-genotoxic hepatocarcinogen in rats, whereas such a property has not been probed in other species.[10] The mechanism of coumarin toxicity has been extensively studied and elucidated; it produces oxidative stress leading to glutathione depletion.[11–13] The species-specific difference between rat and human responses to coumarin has been explained as a difference in detoxification after metabolic activation.[14,15]

In most species, including humans, coumarin is hydroxylated by CYP2A to 7-hydroxycoumarin

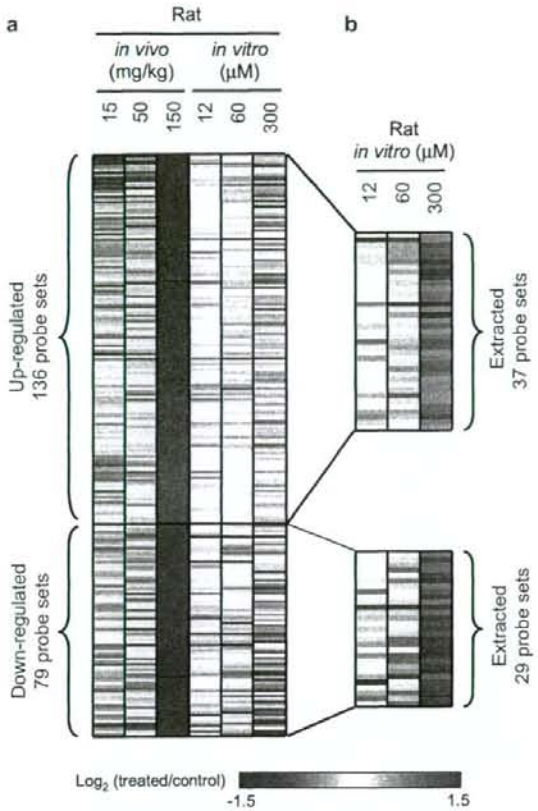

Figure 3 Heatmap of the expression profiles of probe sets in rat liver and rat hepatocytes treated with coumarin. (a) Heatmap of the changes in gene expression induced by coumarin treatment in the in-vivo rat liver (15, 50, 150 mg/kg) and in-vitro hepatocytes (12, 60, and 300 μM). Probes sets were statistically extracted from the data presented in Tables 2 and 3. b: Probe sets with >1.5-fold or <0.6-fold change in rat hepatocytes (the specific sub-set grouped as in-vivo–in-vitro bridging probes are indicated by shading in Tables 2 and 3).

(7-HC), a non-toxic metabolite. In rats, however, CYP2A has a stronger affinity for testosterone than for coumarin, such that 7HC levels are extremely low in this species. Another influencing factor is that in rats, coumarin is converted to coumarin 3,4-epoxide (CE), a reactive intermediate that is detoxified via glutathione conjugation and excreted as a conjugate. When the amount of the active metabolite exceeds the cellular capacity for glutathione conjugation, cell injury may occur. However, there is some evidence to suggest that this pathway is of minor importance to hepatotoxicity, as mouse-liver microsomes show hepatic clearance of coumarin via the epoxide intermediate at levels four times greater than that in rats,[16] but hepatotoxicity is not induced by coumarin treatment in mice. CE is spontaneously converted to another toxic compound, *o*-hydroxyphenylacetaldehyde (*o*-HPA). It has been found that *o*-HPA is rapidly detoxified to *o*-hydroxyphenylacetic acid in mice and humans, whereas this pathway works little in rats.[16,17] Therefore, the difference in *o*-HPA detoxification is currently considered to be the main cause of species-specific differences in sensitivity to coumarin.

The main purpose of the present study was to explore a possible strategy for overcoming the problem of species-specific differences in toxicity that affect testing of potential toxins and therapeutic treatments. Specifically, we were interested to test a toxicogenomics-based approach to address species-specific differences in response to toxins. In the livers of rats treated with coumarin, changes in gene expression were observed in various known genes, possibly reflecting a response to oxidative stress, cell injury, and glutathione depletion, and these coumarin-responsive genes seem likely to be related to the hepatotoxic mechanism of coumarin. Of the coumarin-responsive gene identified in the in-vivo rat liver assay, not all but a considerable numbers of the genes were found to be common to those that were coumarin-responsive in the in-vitro assay, with an observable dose-dependency. The present results suggest that whole-transcriptome analysis of the response can be used to estimate the hepatotoxicity of coumarin using the in-vitro rat hepatocytes. In our experience with other compounds, we found that some chemicals showed a considerably different gene expression profile *in vivo* and *in vitro*,[6] whereas the results with coumarin suggest that it is possible to build a reasonable bridge between rat and human responses using an in-vitro cell assay system.

The responsive genes in common to the in-vivo and in-vitro assay datasets were used to identify human ortholog genes useful for making a comparison between rat and human responses. As it is obvious from the results presented in Figure 4, the trend in changes in expression was similar in both species, but the extent of the changes was generally smaller in human cells than in rat cells in accordance with the known species-specific difference in hepatotoxicity. The observation that induction of stress-related genes and glutathione metabolism–related genes was more robust in rat cells than in human cells could be a direct reflection of the extent of stress and subsequent damage caused by coumarin in each species. The genes "Protein kinase inhibitor p58", "DnaJ (Hsp40) homolog, subfamily B, member 11", "crystallin, lamda 1", "hypoxia up-regulated 1", and "aflatoxin aldehyde reductase" were extensively

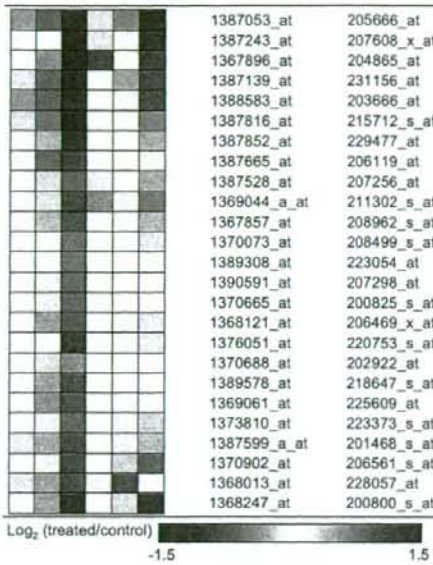

Affymetrix probe ID			
RAE230 2.0	HG-U133 2.0	Gene description (RAE230 2.0)	Gene symbol
1387053_at	205666_at	flavin containing monooxygenase 1	Fmo1
1387243_at	207608_x_at	cytochrome P450, family 1, subfamily A, polypeptide 2	Cyp1a2
1367896_at	204865_at	carbonic anhydrase 3	Ca3
1387139_at	231156_at	hydroxyacid oxidase 2 (long chain)	Hao2
1388583_at	203666_at	chemokine (C-X-C motif) ligand 12	Cxcl12
1387816_at	215712_s_at	insulin-like growth factor binding protein, acid labile subunit	Igfals
1387852_at	229477_at	thyroid hormone responsive protein	Thrsp
1387665_at	206119_at	betaine-homocysteine methyltransferase	Bhmt
1387528_at	207256_at	mannose-binding lectin 2, protein C	Mbl2
1369044_a_at	211302_s_at	phosphodiesterase 4B	Pde4b
1367857_at	208962_s_at	fatty acid desaturase 1	Fads1
1370073_at	208499_s_at	protein kinase inhibitor p58	Dnajc3
1389308_at	223054_at	DnaJ (Hsp40) homolog, subfamily B, member 11	Dnajb11
1390591_at	207298_at	Na/Pi cotransporter 4	Slc17a3
1370665_at	200825_s_at	hypoxia up-regulated 1	Hyou1
1368121_at	206469_x_at	aldo-keto reductase family 7, member A3 (aflatoxin aldehyde reductase)	Akr7a3
1376051_at	220753_s_at	crystallin, lamda 1	Cryl1
1370688_at	202922_at	glutamate-cysteine ligase, catalytic subunit	**Gclc**
1389578_at	218647_s_at	ischemia/reperfusion inducible protein	Yrdc
1369061_at	225609_at	glutathione reductase	Gsr
1373810_at	223373_s_at	phospholipase A2, group XIIA (predicted)	Pla2g12a
1387599_a_at	201468_s_at	NAD(P)H dehydrogenase, quinone 1	Nqo1
1370902_at	206561_s_at	aldo-keto reductase family 1, member B8	Akr1b8
1368013_at	228057_at	DNA-damage-inducible transcript 4-like	**Ddit4l**
1368247_at	200800_s_at	heat shock 70kD protein 1A/1B	**Hspa1a/1b**

Figure 4 Heatmap of the expression profile of probe sets in rat and human hepatocytes treated with coumarin. Among the set of in-vivo–in-vitro bridging probes for rats, 14 up-regulated and 11 down-regulated probe sets were assigned human orthologs (species bridging markers) and their expression is shown as a heatmap that includes the expression profiles in rat and human hepatocytes treated with 12, 60, or 300 μM coumarin. Note that each probe set responded dose-dependently to coumarin in both species, whereas the extent of the changes appears to be more prominent in rat than in human cells.

up-regulated in rats both *in vivo* and *in vitro*, whereas almost no change was observed in these genes in human hepatocytes. It will likely be interesting to determine if the gene sets include genes involved in the cause of the species-specific responses that lead to differences in hepatotoxicity and those genes not involved in the response to coumarin. Clearly, it will be necessary to perform additional experiments to address this question.

We next explored the utility of a score, the TGP2-score that is aimed at quantifying responsiveness of a set of marker genes. The TGP2-score is the average of the effect size on gene expression. When species-specific differences in drug-induced gene expression changes are examined, we often encounter clusters of genes, possibly related to toxicological function, that are affected by the drug in both species tested but in different directions (i.e., up-regulated in one but down-regulated in the other). If responsiveness is quantified by taking account of the direction of changes, we might underestimate the extent to which the set of genes affected are similar. Using the TGP2-score, we estimate responsiveness of a given species when expression of a gene in the analysis set is mobilized in either direction. In the present case, however, the direction of expression change was in common between two species in most or all cases, such that the factor did not contribute much to the scores. The score is also clearly useful to visualize quantitative responsiveness of a set of genes to a toxicant (Figure 5) and a prediction of species-specific difference can also be represented (i.e., the higher toxicity of coumarin in rat than in humans or the lack of a species-specific difference in the case of toxicity of DFNa; Figure 5). It also follows that the genes selected in this study may be useful in-vitro markers of oxidative stress–related hepatocyte injury in both rats and humans and that differential responses in these marker genes are indicative of a species-specific difference.

In conclusion, we successfully used a toxicogenomics approach to reproduce the known species-specific difference in hepatotoxicity of coumarin between rats and humans using an in-vitro hepatocyte culture system and microarray analysis. The application of this approach to other chemicals in our database should reveal other examples that can build bridges between species or suggest other strategies for bridging information among species. The most important mission for a toxicologist interested

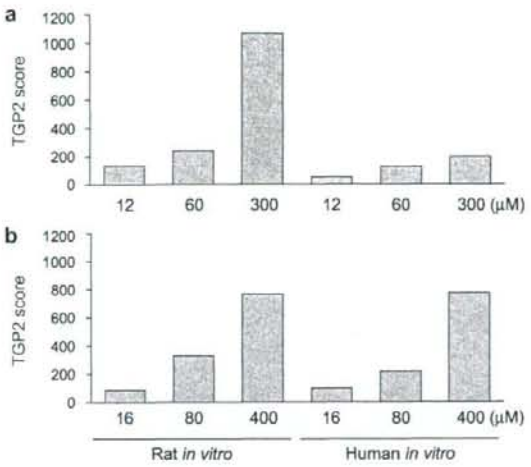

Figure 5 The responsiveness of rat and human hepatocytes expressed as a score based on the effect size (TGP2 score). The expression of each probe set in the set of rat–human bridging probes (Figure 4) was converted to a TGP2 score as described in "Materials and methods" to quantify the responsiveness of each species. (a) Responsiveness to coumarin. Note that the score shows a clear dose-dependency and the expected species-specific difference, that is, rat hepatocytes are more sensitive than human hepatocytes. (b) Responsiveness to diclofenac sodium, a known hepatotoxicant that causes oxidative stress but does not show a species-specific difference in hepatotoxicity. Again, a dose-dependent increase in the score is observed but in this case, as expected, no species-specific difference is observed.

in drug development is to make a precise prediction of the potential clinical toxicity based on animal studies. Toxicogenomics-based approaches are emerging as a promising new avenue of study for making the most of the results of animal studies.

Acknowledgement

This study was supported by a grant from the Ministry of Health, Labour and Welfare of Japan (H14-toxico-001).

References

1 Urushidani, T, Nagao, T. Toxicogenomics: the Japanese initiative. In: Borlak, J, (Ed.), *Handbook of toxicogenomics – strategies and applications. Wiley: VCH*; 2005. p. 623–31.
2 Takashima, K, Mizukawa, Y, Morishita, K, Okuyama, M, Kasahara, T, Toritsuka, N, *et al.* Effect of the difference in vehicles on gene expression in the rat liver-analysis of the control data in the Toxicogenomics Project Database. *Life Sci* 2006; **78**: 2787–2796.
3 Waters, MD, Fostel, JM. Toxicogenomics and systems toxicology: aims and prospects. *Nat Rev Genet* 2004; **5**: 936–948.
4 Mattingly, CJ, Colby, GT, Forrest, JN, Boyer, JL. The Comparative Toxicogenomics Database (CTD). *Environ Health Perspect* 2003; **111**: 793–795.
5 Liu, G, Loraine, AE, Shigeta, R, Cline, M, Cheng, J, Valmeekam, V, *et al.* NetAffx: Affymetrix probesets and annotations. *Nucleic Acids Res* 2003; **31**: 82–86.
6 Kiyosawa, N, Shiwaku, K, Hirode, M, Omura, K, Uehara, T, Shimizu, T, *et al.* Utilization of a one-dimensional score for surveying chemical-induced changes in expression levels of multiple biomarker gene sets using a large-scale toxicogenomics database. *J Toxicol Sci* 2006; **31**: 433–448.
7 Hedges, LV. Distribution theory for Glass's estimator of effect size and related estimators. *J Edu Statis* 1981; **6**: 107–128.
8 Gomez-Lechon, MJ, Ponsoda, X, O'Connor, E, Donato, T, Castell, JV, Jover, R. Diclofenac induces apoptosis in hepatocytes by alteration of mitochondrial function and generation of ROS. *Biochem Pharmacol* 2003; **66**: 2155–2167.
9 Amin, A, Hamza, AA. Oxidative stress mediates drug-induced hepatotoxicity in rats: a possible role of DNA fragmentation. *Toxicology* 2005; **208**: 367–375.
10 National Toxicology Program. NTP toxicology and carcinogenesis studies of coumarin (CAS No. 91-64-5) in F344/N rats and B6C3F1 mice (Gavage Studies). *Natl Toxicol Program Tech Rep Ser* 1993; **422**: 1–340.
11 Lake, BG. Investigations into the mechanism of coumarin-induced hepatotoxicity in the rat. *Arch Toxicol Suppl* 1984; **7**: 16–29.
12 Lake, BG, Gray, TJ, Evans, JG, Lewis, DF, Beamand, JA, Hue, KL. Studies on the mechanism of coumarin-induced toxicity in rat hepatocytes: comparison with dihydrocoumarin and other coumarin metabolites. *Toxicol Appl Pharmacol* 1989; **97**: 311–323.
13 Kiyosawa, N, Uehara, T, Gao, W, Omura, K, Hirode, M, Shimizu, T, *et al.* Identification of glutathione depletion-responsive genes using phorone-treated rat liver. *J Toxicol Sci* 2007; **32**: 469–486.
14 Vassallo, JD, Hicks, SM, Daston, GP, Lehman-McKeeman, LD. Metabolic detoxification determines species differences in coumarin-induced hepatotoxicity. *Toxicol Sci* 2004; **80**: 249–257.
15 Felter, SP, Vassallo, JD, Carlton, BD, Daston, GP. A safety assessment of coumarin taking into account species-specificity of toxicokinetics. *Food Chem Toxicol* 2006; **44**: 462–475.
16 Born, SL, Hu, JK, Lehman-McKeeman, LD. o-hydroxyphenylacetaldehyde is a hepatotoxic metabolite of coumarin. *Drug Metab Dispos* 2000a; **28**: 218–223.
17 Born, SL, Caudill, D, Smith, BJ, Lehman-McKeeman, LD. In vitro kinetics of coumarin 3,4-epoxidation: application to species differences in toxicity and carcinogenicity. *Toxicol Sci* 2000b; **58**: 23–31.

Available online at www.sciencedirect.com
ScienceDirect
Toxicology and Applied Pharmacology 229 (2008) 290–299
Toxicology and Applied Pharmacology
www.elsevier.com/locate/ytaap

Gene expression profiling in rat liver treated with compounds inducing phospholipidosis

Mitsuhiro Hirode [a,b], Atsushi Ono [b,c], Toshikazu Miyagishima [b], Taku Nagao [d], Yasuo Ohno [c], Tetsuro Urushidani [b,e,*]

[a] Development Research Center, Pharmaceutical Research Division, Takeda Pharmaceutical Company Limited, Yodogawa-ku, Osaka, 532-8686, Japan
[b] Toxicogenomics Project, National Institute of Biomedical Innovation, Ibaraki, Osaka, 567-0085, Japan
[c] National Institute of Health Sciences, Setagaya-ku, Tokyo 158-8501, Japan
[d] Food Safety Commission of Japan, Chiyoda-ku, Tokyo, 100-8989, Japan
[e] Department of Pathophysiology, Doshisha Women's College of Liberal Arts, Kyotanabe, Kyoto 610-0395, Japan

Received 27 October 2007; revised 14 January 2008; accepted 19 January 2008
Available online 14 February 2008

Abstract

We have constructed a large-scale transcriptome database of rat liver treated with various drugs. In an effort to identify a biomarker for diagnosis of hepatic phospholipidosis, we extracted 78 probe sets of rat hepatic genes from data of 5 drugs, amiodarone, amitriptyline, clomipramine, imipramine, and ketoconazole, which actually induced this phenotype. Principal component analysis (PCA) using these probes clearly separated dose- and time-dependent clusters of treated groups from their controls. Moreover, 6 drugs (chloramphenicol, chlorpromazine, gentamicin, perhexiline, promethazine, and tamoxifen), which were reported to cause phospholipidosis but judged as negative by histopathological examination, were designated as positive by PCA using these probe sets. Eight drugs (carbon tetrachloride, coumarin, tetracycline, metformin, hydroxyzine, diltiazem, 2-bromoethylamine, and ethionamide), which showed phospholipidosis-like vacuolar formation in the histopathology, could be distinguished from the typical drugs causing phospholipidosis. Moreover, the possible induction of phospholipidosis was predictable by the expression of these genes 24 h after single administration in some of the drugs. We conclude that these identified 78 probe sets could be useful for diagnosis of phospholipidosis, and that toxicogenomics would be a promising approach for prediction of this type of toxicity.
© 2008 Elsevier Inc. All rights reserved.

Keywords: Phospholipidosis; Toxicogenomics; Rat; Liver; Principal component analysis

Introduction

The toxicogenomics project was a 5-year collaborative project by the National Institute of Biomedical Innovation (NIBIO), the National Institute of Health Science (NIHS), and 15 pharmaceutical companies in Japan that started in 2002 (Urushidani and Nagao, 2005). Its aim was to construct a large-scale toxicology database of transcriptome for prediction of toxicity of new chemical entities in the early stage of drug development. About 150 chemicals, mainly medicinal compounds, were selected, and gene expression in liver (also kidney in some cases) was comprehensively analyzed by using Affymetrix GeneChip®. In 2007, the project was finished and the whole system, consisting of the database, the analyzing system and the prediction system, was completed and named as TG-GATEs (Genomics Assisted Toxicity Evaluation System developed by the Toxicogenomics Project, Japan). The present mission is to identify potential biomarker gene lists useful for prediction or diagnosis of drug-induced hepato- and nephro-toxicity using this system.

In toxicity studies, phospholipidosis (PLsis) is often observed in various tissues including liver, kidney, and lung. PLsis is a lipid storage disease characterized by intracellular accumulation of phospholipids and the appearance of membranous lamellar inclusions known as lamellar bodies. Its pathogenesis has been thought to be the unbalance of phospholipid turnover. As for drug-induced PLsis, it is well known that cationic

* Corresponding author. Department of Pathophysiology, Doshisha Women's College of Liberal Arts, Kyotanabe, Kyoto 610-0395, Japan. Fax: +81 774 65 8689.
E-mail address: turushid@dwc.doshisha.ac.jp (T. Urushidani).

0041-008X/$ - see front matter © 2008 Elsevier Inc. All rights reserved.
doi:10.1016/j.taap.2008.01.036

amphiphilic drugs (CADs), characterized by a hydrophobic ring structure and a hydrophilic side chain with a charged amine group have the potential to cause PLsis. Therefore, it has been postulated that drug-induced PLsis involves direct binding of CADs to phospholipids, subsequently creating a complex that is resistant to degradation by phospholipases (Reasor et al., 2006). There is also an observation that some CADs can cause PLsis by directly inhibiting phospholipase activity (Halliwell, 1997; Reasor et al., 2006). Although much effort has been done to establish the methods to predict PLsis of drugs (Tomizawa et al., 2006), sensitive diagnostic markers and effective prognostic markers are still desired.

In the present study, we selected PLsis in liver as a target phenotype, and tried to identify candidate biomarkers that enable the cell to discriminate chemicals with the potential to cause this phenotype for application of TG-GATEs.

Materials and methods

Compounds. Compounds used for the data analysis are listed in Table 1, in which the chemical name, abbreviation, dosage, administration route and vehicle used in the study are summarized.

Animal treatment. The experiments were carried out as previously described in the literature (Takashima et al., 2006). Male Crl:CD(SD) rats were purchased from Charles River Japan Inc., (Kanagawa, Japan) at 5-weeks of age. After a 7-day quarantine and acclimatization period, the animals were divided into groups of 5 animals using a computerized stratified random grouping method based on body weight for each age. The animals were individually housed in stainless-steel cages in a room that was lighted for 12 h (7:00–19:00) daily, ventilated with an air-exchange rate of 15 times per hour, and maintained at 21–25 °C with a relative humidity of 40–70%. Each animal was allowed free access to water and pellet food (CRF-1, sterilized by radiation, Oriental Yeast Co., Japan). Rats in each group were orally administered with various drugs suspended or dissolved either in 0.5% methylcellulose solution (MC) or corn oil according to their dispersibility, except for gentamicin and 2-bromoethylamine, which were dissolved in saline and administered intravenously. The animals were treated for 3, 7, 14 or 28 days and sacrificed 24 h after the last dosing. Blood samples were collected to a heparinized tube under ether anesthesia from the abdominal aorta after which the animals were euthanized.

The experimental protocols were reviewed and approved by the Ethics Review Committee for Animal Experimentation of the National Institute of Health Sciences.

Microarray analysis. After collecting the blood, the animals were euthanized by exsanguination from the abdominal aorta under ether anesthesia. An aliquot of the sample (about 30 mg) for RNA analysis was obtained from the left lateral lobe of the liver in each animal immediately after termination, kept in RNAlater® (Ambion, Austin, TX, USA) overnight at 4 °C, and then frozen at −80 °C until use. Liver samples were homogenized with the buffer RLT supplied in RNeasy Mini Kit (Qiagen, Valencia, CA, USA), and total RNA was isolated according to the manufacturer's instructions. Microarray analysis was conducted on 3 out of 5 samples for each group by using GeneChip® Rat Genome 230 2.0 Arrays (Affymetrix, Santa Clara, CA, USA), containing 31,042 probe sets. The procedure was conducted basically according to the manufacturer's instructions using Superscript Choice System (Invitrogen, Carlsbad, CA, USA) and T7-(dT)24-oligonucleotide primer (Affymetrix) for cDNA synthesis, cDNA Cleanup Module (Affymetrix) for purification, and BioArray High yield RNA Transcript Labeling Kit (Enzo Diagnostics, Farmingdale, NY, USA) for synthesis of biotin-labeled cRNA. Ten micrograms of fragmented cRNA was hybridized to a Rat Genome 230 2.0 Array for 18 h at 45 °C at 60 rpm, after which the array was washed and stained by streptavidin–phycoerythrin using Fluidics Station 400 (Affymetrix) and scanned by Gene Array Scanner (Affymetrix). The digital image files were processed by Affymetrix Microarray Suite version 5.0. Microarray image data were analyzed with GeneChip Operating Software (Affymetrix).

The digital image files were processed by Affymetrix Microarray Suite version 5.0 and the intensities were normalized for each chip by setting the mean intensity to 500 (per chip normalization).

Statistical analysis. In order to extract probe sets related to PLsis, we first employed gene expression data of rat liver treated with repeated administration for 3, 7, 14, and 28 days of AM, AMT, CPM, IMI and KC in our database, and they are known to cause PLsis, and in fact, the induction of this disease was confirmed in the present study.

After removing the probe sets with Affymetrix absent call in the whole 48 sample set ($N=3$ for 4 time points and 4 dose levels for one drug), differentially

Table 1
Compounds

Compound name	Abbreviation	Dose (dose level, mg/kg)			Administration route	Vehicle
		Low	Middle	High		
Amiodarone	AM	200/20*	600/60*	2000/200*	PO	MC
Amitriptyline	AMT	15	50	150	PO	MC
Clomipramine	CPM	10	30	100	PO	MC
Imipramine	IMI	10	30	100	PO	MC
Ketoconazole	KC	10	30	100	PO	MC
Chloramphenicol	CMP	100	300	1000	PO	MC
Chlorpromazine	CPZ	4.5	45/15*	150/45*	PO	MC
Gentamicin	GMC	10	30	100	IV	SA
Perhexiline	PH	15	50	150	PO	MC
Promethazine	PMZ	20	60	200	PO	MC
Tamoxifen	TMX	6	20	60	PO	CO
Carbon tetrachloride	CCl4	30	100	300	PO	CO
Coumarin	CMA	15	50	150	PO	CO
Tetracycline	TC	100	300	1000	PO	MC
Metformin	MFM	100	300	1000	PO	MC
Hydroxyzine	HYZ	10	30	100	PO	MC
Diltiazem	DIL	80	240	800	PO	MC
2-bromoethylamine	BEA	6/2*	20/6*	60/20*	IV	SA
Ethionamide	ETH	100/30*	300/100*	1000/300*	PO	MC

*: as single dose/repeated dose.
PO: peroral, IV: intravenous.
MC: 0.5 w/v% methylcellulose; SA: saline; CO: corn oil.

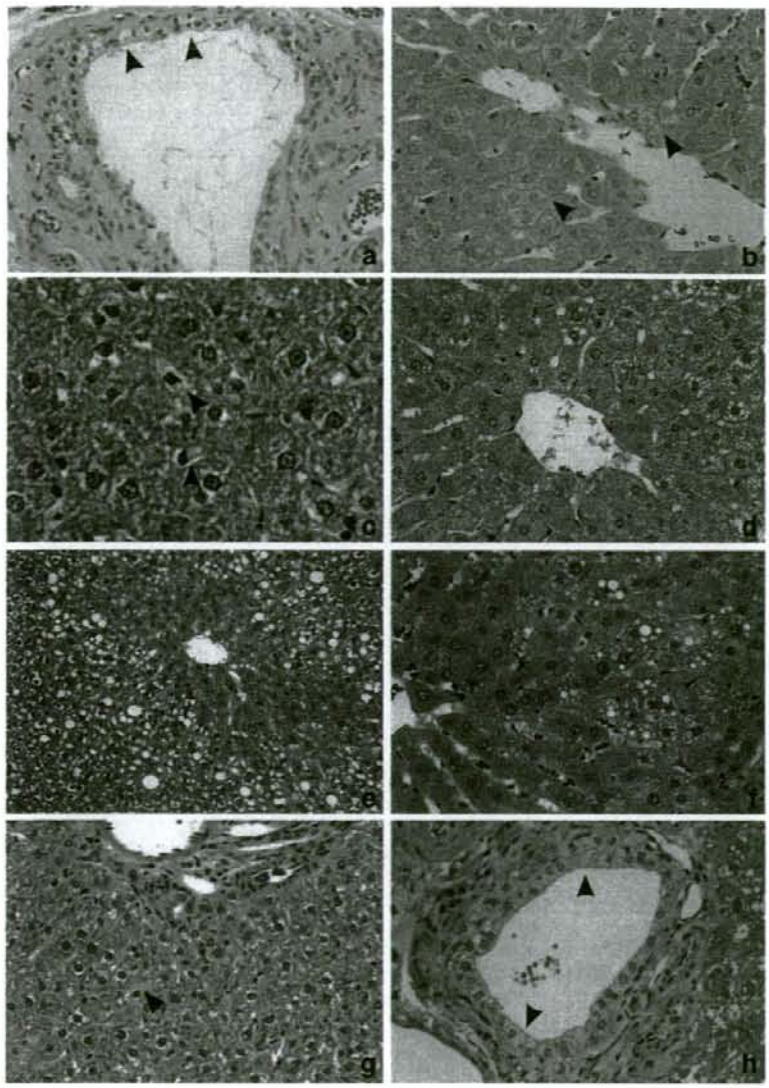

Fig. 1. Histopathology of rat liver treated with amiodarone, amitriptyline, clomipramine, imipramine, and ketoconazole. a–c. Amiodarone 200 mg/kg, 29th day. Vacuolations in the bile duct cell (a) in the hepatocyte (b) and in the Kupffer cell (c) are evident (arrowheads). d. Amitriptyline 150 mg/kg, 29th day. Vacuolation in the hepatocyte is evident. e. Clomipramine 100 mg/kg, 29th day. Vacuolation is noted in the midlobular hepatocytes. f–g. Imipramine 100 mg/kg, 29th day. Vacuolations in the hepatocyte (f) and in the Kupffer cell (g) are evident. h. Ketoconazole 100 mg/kg, 29th day. Vacuolation occurs exclusively in the bile duct (arrowheads).

expressed genes by the treatment were extracted by Welch's ANOVA ($p<0.05$) for the dose level at any time point. This procedure was continued for 4 time points and genes showing significant change, and any points were combined as PLsis responsive genes. In the next step, commonly mobilized genes among these 5 chemicals were selected.

Principal component analysis (PCA) of the GeneChip data was also performed using Spotfire DecisionSite.

Pathway and gene ontology (GO) analysis. The identified probe sets were subjected to analysis of Kyoto Encyclopedia of Genes and Genomes (KEGG) pathway and GO analysis by DAVID (Database for Annotation, Visualization, and Integrated Discovery; http://apps1.niaid.nih.gov/david/ using Fisher's exact test (Dennis et al., 2003). Level 5 analysis was adopted.

Results

Histopathological examination

The results of histopathological examination of 5 compounds (AM, AMT, CPM, IMI and KC) known to induce PLsis are shown in Fig. 1 and Table 2. For most cases, clear vacuolization was observed in the cytoplasm of hepatocytes, and this change tended to progress with dose and time. Vacuolation was also noted in Kupffer cell (AM, IMI) or bile duct (AM). In the case of KC, vacuolation occurred exclusively in the bile duct.

Table 2
Histopathological findings

Compound	Findings	Time	Dose		
			Low	Middle	High
AM	Vacuolization, bile duct cell	3 h–4 day	–	–	–
		8 day	–	–	3/5(±)
		15 day	–	–	1/5(±), 4/5(+)
		29 day	–	–	4/4(+)
	Vacuolization, hepatocyte	3 h–8 day	–	–	–
		15 day	–	–	2/5(±)
		29 day	–	–	4/4(±)
	Vacuolization, Kupffer cell	3 h–8 day	–	–	–
		15 day	–	–	5/5(±)
		29 day	–	–	4/4(±)
AMT	Vacuolization, hepatocyte	3 h–4 day	–	–	–
		8 day	–	–	4/5(±)
		15 day	–	1/5(±)	5/5(+)
		29 day	–	1/5(±), 2/5(+)	1/3(+), 2/3(2+)
CPM	Vacuolization, hepatocyte	3 h–15 day	–	–	–
		29 day	–	–	1/5(±), 1/5(+)
IMI	Vacuolization, hepatocyte	3 h–4 day	–	–	–
		8 day	–	–	4/5(±)
		15 day	–	–	1/5(±), 2/5(+)
		29 day	–	2/5(±)	1/4(±), 3/4(+)
	Vacuolization, Kupffer cell	3 h–8 day	–	–	–
		15 day	–	–	3/5(±)
		29 day	–	–	–
KC	Vacuolization, bile duct cell	3 h–24 h	–	–	–
		4 day	–	–	5/5(+)
		8 day	–	–	5/5(+)
		15 day	–	1/5(+)	2/5(+), 3/5(2+)
		29 day	–	1/5(±), 4/5(+)	5/5(2+)
CMP	Abnormality	3 h–29 day	–	–	–
CPZ	Abnormality	3 h–29 day	–	–	–
GMC	Abnormality	3 h–29 day	–	–	–
PH	Abnormality	3 h–29 day	–	–	–
PMZ	Abnormality	3 h–29 day	–	–	–
TMX	Abnormality	3 h–29 day	–	–	–
CCl4	Degeneration, fatty, hepatocyte	3 h–9 h	–	–	–
		24 h	–	2/5(±)	1/5(±), 4/5(+)
		4 day	4/5(±), 1/5(+)	5/5(+)	1/5(±), 4/5(+)
		8 day	1/5(±), 4/5(+)	5/5(+)	4/5(+), 1/5(2+)
		15 day	1/5(±), 4/5(+)	5/5(+)	4/5(+), 1/5(2+)
		29 day	5/5(+)	4/5(+), 1/5(2+)	2/5(+), 2/5(2+), 1/5(3+)
CMA	Vacuolization, hepatocyte	3 h–8 day	–	–	–
		15 day	–	–	2/5(±), 1/5(+)
		29 day	–	–	5/5(+)
TC	Vacuolization, hepatocyte	3 h–8 day	–	–	–
		15 day	–	–	2/5(±)
		29 day	–	–	2/5(±)
MFM	Deposit, glycogen, hepatocyte	3 h–24 h	–	–	–
		4 day	–	2/5(±)	5/5(±)
		8 day	–	–	2/5(±)
		15 day	–	–	2/5(±)
		29 day	–	–	1/5(±)
HYZ	Vacuolization, hepatocyte	3 h–8 day	–	–	–
		15 day	–	–	2/5(±), 2/5(+)
		29 day	–	–	4/5(+), 1/5(2+)
DIL	Vacuolization, hepatocyte	3 h–4 day	–	–	–
		8 day	–	–	2/5(±)
		15 day	–	1/5(±)	5/5(±)
		29 day	–	4/5(±)	4/4(±)
BEA	Vacuolization, hepatocyte	3 h–8 day	–	–	–
		15 day	–	–	2/5(+)
		29 day	–	4/5(+)	4/5(+)
ETH	Vacuolization, hepatocyte	3 h–24 h	–	–	–
		4 day	–	4/5(+), 1/5(2+)	5/5(+)
		8 day	–	3/5(±), 2/5(+)	3/3(+)
		15 day	–	2/5(±), 3/5(+)	2/5(±), 3/5(+)
		29 day	–	2/5(+)	NA

–: not remarkable, ±: minimal,+: mild, 2+: moderate, 3+: severe, NA: not applicable.

Microarray data analysis

Differentially expressed genes with statistical significance were extracted from each of 5 representative drugs inducing PLsis, as described in the Materials and methods section. The numbers of extracted probe sets were 4915 for AM, 3565 for AMT, 1907 for CPM, 2339 for IMI, and 3482 for KC. We then selected the probe sets that were commonly changed in all compounds and 78 probe sets were obtained. The list of these probe sets is shown in Table 3. Based on gene ontology, the contents of genes related to carboxylic acid metabolism, electron transport, amino acid metabolism, amine catabolism, and nitrogen compound catabolism were significantly high (Table 4). Although not significant, 4 lipid biosynthesis-related genes were contained. This feature might reflect the cellular changes related to lipid metabolism in association with PLsis.

Principal component analysis (PCA)

Using the 78 probe sets extracted as above, PCA was performed on the 5 drugs inducing PLsis. As shown in Fig. 2,

Table 3
List of 78 probe sets changed in 5 compounds inducing PLsis

Probe set ID	Gene title	Gene symbol
1367676_at	High mobility group box 2	Hmgb2
1367819_at	Glutamate oxaloacetate transaminase 2, mitochondrial	Got2
1368016_at	Peroxisomal *trans*-2-enoyl-CoA reductase	Pecr
1368171_at	Lysyl oxidase	Lox
1368213_at	P450 (cytochrome) oxidoreductase	Por
1368275_at	Sterol-C4-methyl oxidase-like	Sc4mol
1368403_at	Retinoblastoma-like 2	Rbl2
1368467_at	Cytochrome P450, family 4, subfamily F, polypeptide 2	Cyp4f2
1368520_at	Apolipoprotein A-IV	Apoa4
1368618_at	Growth factor receptor bound protein 14	Grb14
1368718_at	Aldehyde dehydrogenase family 1, subfamily A4	Aldh1a4
1368778_at	Solute carrier family 6 (neurotransmitter transporter, taurine), member 6	Slc6a6
1368905_at	Carboxylesterase 2 (intestine, liver)	Ces2
1368931_at	SH3-domain GRB2-like 3	Sh3gl3
1368977_a_at	Fractured callus expressed transcript 1	Fxc1
1369275_s_at	Cytochrome P450 IIA1 (hepatic steroid hydroxylase IIA1) gene	Cyp2a1
1369737_at	cAMP responsive element modulator	Crem
1369850_at	UDP-glucuronosyltransferase 2 family, polypeptide A1	Ugt2a1
1370004_at	H2A histone family, member Y	H2afy
1370054_at	Cyclin-dependent kinase inhibitor 2C (p18, inhibits CDK4)	Cdkn2c
1370375_at	Glutaminase 2 (liver, mitochondrial)	Gls2
1370583_s_at	ATP-binding cassette, subfamily B (MDR/TAP), member 1	Abcb1
1370613_s_at	UDP glycosyltransferase 1 family, polypeptide A1	Ugt1a1
1370698_at	Liver UDP-glucuronosyltransferase, phenobarbital-inducible form liver	Udpgtr2
1371076_at	Cytochrome P450, family 2, subfamily b, polypeptide 15	Cyp2b15
1371089_at	Transcribed locus	–
1371412_a_at	Neuronal regeneration related protein	Nrep
1371546_at	Similar to TR4 orphan receptor-associated protein TRA16	LOC361128
1371680_at	Similar to gamma-aminobutyric acid (GABA(A)) receptor-associated protein-like 1	LOC683917
1371809_at	Mitochondrial ribosomal protein S18B	Mrps18b
1371875_at	Mannosidase, beta A, lysosomal	Manba
1372056_at	CKLF-like MARVEL transmembrane domain containing 6	Cmtm6
1372124_at	Eukaryotic translation initiation factor 4B	Eif4b
1372181_at	Similar to expressed sequence AA408877	RGD1308513
1372479_at	Transcribed locus, moderately similar to NP_064456.1 fibrinogen, beta polypeptide [*Rattus norvegicus*]	–
1372602_at	Similar to genethonin 1	RGD1311800
1372885_at	Transcribed locus	–
1373015_at	Ring finger protein 11 (predicted)	Rnf11_predicted
1373626_at	Transcribed locus	–
1373823_at	Similar to cyclin-dependent kinases regulatory subunit 2 (CKS-2) (predicted)	RGD1562047_predicted
1373924_at	Similar to C530044N13Rik protein	RGD1306568
1373970_at	Similar to RIKEN cDNA 9230117N10	RGD1311155
1374531_at	Transcribed locus	–
1374953_at	Similar to CG12279-PA	LOC500420
1375423_at	MAX-like protein X	Mlx
1375637_at	Similar to RIKEN cDNA 1110003E01	RGD1311122
1375909_at	Similar to glutathione transferase GSTM7-7	MGC108896
1377019_at	Transcribed locus	–
1378016_at	Echinoderm microtubule associated protein-like 4 (predicted)	Eml4_predicted
1380254_at	Transcribed locus, moderately similar to NP_079928.1 general transcription factor III A [*Mus musculus*]	–
1384169_a_at	Vav2 oncogene (predicted)	Vav2_predicted
1386857_at	Stathmin 1	Stmn1
1386917_at	Pyruvate carboxylase	Pc
1387006_at	Rat senescence marker protein 2A gene, exons 1 and 2	Smp2a
1387022_at	Aldehyde dehydrogenase family 1, member A1	Aldh1a1
1387031_at	Endoplasmic reticulum protein 29	Erp29
1387093_at	Solute carrier organic anion transporter family, member 1a4	Slco1a4
1387094_at	Solute carrier organic anion transporter family, member 1a4	Slco1a4
1387109_at	P450 (cytochrome) oxidoreductase	Por
1387118_at	Cytochrome P450, family 3, subfamily a, polypeptide 1	Cyp3a1
1387203_at	Glucokinase regulatory protein	Gckr
1387223_at	Aminoadipate aminotransferase	Aadat

Table 3 (*continued*)

Probe set ID	Gene title	Gene symbol
1387307_at	Histidine ammonia lyase	Hal
1387511_at	Cytochrome P450 IIA1 (hepatic steroid hydroxylase IIA1) gene	Cyp2a1
1387665_at	Betaine-homocysteine methyltransferase	Bhmt
1387669_a_at	Epoxide hydrolase 1, microsomal	Ephx1
1387759_s_at	UDP glycosyltransferase 1 family, polypeptide A1	Ugt1a1
1387793_at	Transcribed locus, strongly similar to NP_075738.1 yippee-like 1 [*Mus musculus*]	–
1388212_a_at	RT1 class Ib, locus S3	RT1-S3
1388348_at	Transcribed locus	–
1388425_at	Similar to RIKEN cDNA D130038B21	RGD1305890
1388874_at	Metastasis suppressor 1 (predicted)	Mtss1_predicted
1389319_at	Similar to endoplasmic reticulum-Golgi intermediate compartment protein 1 (ER-Golgi intermediate compartment 32 kDa protein) (ERGIC-32)	LOC287177
1389557_at	Testis expressed gene 261	Tex261
1389986_at	CDNA clone IMAGE:7321089	–
1390455_at	Abhydrolase domain containing 2 (predicted)	Abhd2_predicted
1398754_at	Ubiquitin A-52 residue ribosomal protein fusion product 1	Uba52
1398848_at	Suppression of tumorigenicity 13	St13

treated samples were dose-dependently separated to form clusters from controls, mainly toward the direction of PC1 (contribution rate: 34.8%). In order to examine the time-dependency, all the samples were aligned on a one dimensional graph of PC1 (Fig. 3). It appears that the PC1 value generally increased with time as well as with a dose of these drugs. In case of KC, time- and dose-dependency were obscure, although the treated group clearly formed a cluster separated from the control cluster. Of the genes contributing to PC1, those with high eigenvector value were listed in Table 5. We noticed that the top 4 genes are cytochrome oxidoreductase, sterol-C4-methy oxidase-like, aldehyde dehydrogenase 1A4, and carboxylesterase 2, which are all involved in lipid metabolism.

Distinction of 6 compounds reported to induce PLsis with no abnormality in present histopathological examination

In a survey of the literature, in addition to the 5 drugs above, 6 more drugs, i.e., CMP, CPZ, GMC, PH, PMZ, and TMX in our database, are reported to induce PLsis, but no such histopathological abnormalities were confirmed in the present examination. We then applied PCA using the 78 probe sets on these 6 drugs and we show the results in Fig. 4 as a one dimensional graph with PC1. It was revealed that these 6 drugs were also separated from control clusters the same way as the 5 typical drugs inducing PLsis. Of these, some drugs such as CPZ, GMC and PH, did not change their position very much, but their extent was roughly equivalent to that of KC.

Table 4
GO analysis of identified 78 probe sets

Term	Count	Percent	*P*-value
Carboxylic acid metabolism	10	11.5	1.90E–04
Electron transport	6	6.9	1.20E–02
Amino acid metabolism	5	5.7	1.80E–02
Amine catabolism	3	3.4	3.20E–02
Nitrogen compound catabolism	3	3.4	3.40E–02
Lipid biosynthesis	4	4.6	6.10E–02

Distinction of 8 compounds showing pathological changes similar to PLsis

When examination by light microscope of HE-stained specimens is performed, we sometimes encounter a phenotype (not PLsis but another pathological change), such as lipidosis, deposition of glycogen, or hydropic degeneration, and they are quite difficult to distinguish from each other. In our database, we identified 8 drugs (CCL4, CMA, TC, MFM, HYZ, DIL, BEA, and ETH) showing such pathological changes in liver. The histopathological description of each was as follows: CCL4: "degeneration, fatty, hepatocyte"; CMA, TC, HYZ, DIL, BEA, ETH: "vacuolization, hepatocyte"; and MFM: "deposit, glycogen, hepatocyte". To examine the efficiency of the 78 probe sets, PCA was applied to these 8 pseudo-positive compounds.

As shown in Fig. 5, most of the treated samples stayed in the position close to that of the control samples. Exceptionally, HYZ and DIL formed separate clusters from the controls, as 5 standard compounds inducing PLsis.

Possible distinction of the samples 24 h after a one time dosage

The above results clearly suggested that the list of extracted 78 probe sets was a useful diagnostic marker for PLsis in rat liver. The next question is whether the list works as a prognostic marker for PLsis. To examine this possibility, we performed PCA using the list for the gene expression profile 24 h after the single dose, and practically no pathological changes had occurred at that time. As shown in Fig. 6 left, AM 20, 60, and 200 mg/kg had a high PC1 value in repeated administration for 3 days or more, whereas that in the single dose group was close to the cluster of the control group. Then we additionally performed single dose experiments using higher doses, i.e., 200,

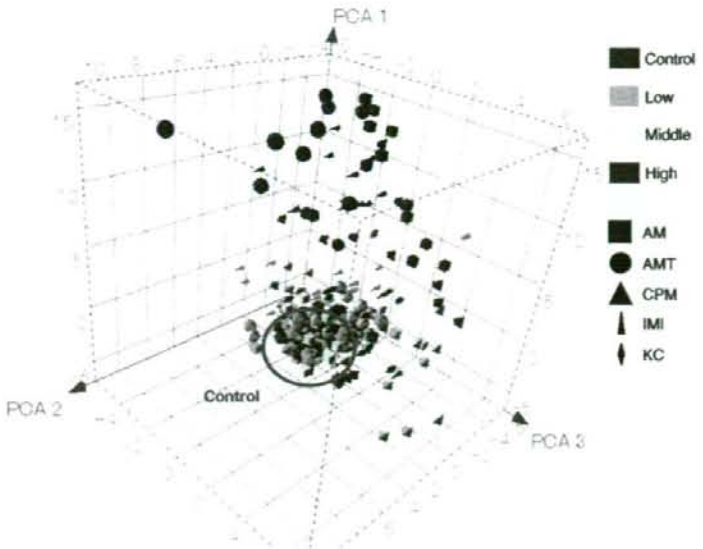

Fig. 2. Principal component analysis of gene expression profiles of amiodarone (AM), amitriptyline (AMT), clomipramine (CPM), imipramine (IMI), and ketoconazole (KC) that induced phospholipidosis in liver in the present study using the commonly mobilized 78 probe sets. Results are expressed as a three dimensional figure with PC1, 2, and 3. Treated samples were dose-dependently separated from the cluster of controls (circled by a blue line), mainly toward the direction of PC1 (contribution rate: 34.8%). For simplicity, rats receiving the same dose with different durations (3, 7, 14 and 28 days, N=3 for each; 12 total) were expressed by the same symbol.

600, and 2000 mg/kg of AM (Fig. 6, right). It was revealed that the group receiving a single dose of 2000 mg/kg AM clustered at a position clearly higher than controls with equivalent PCA1 values receiving a repeated dose of 200 mg/kg for 3 days. In the case of CPZ, the samples at 24 h after the 45 mg/kg single dosing were clearly separated from control samples to an extent more than that of the repeated dose samples (Fig. 7). We then performed additional single dose experiments using 45 and 150 mg/kg CPZ. It was clear from Fig. 7 that 150 mg/kg CPZ showed a higher PC1 value than the 45 mg/kg group.

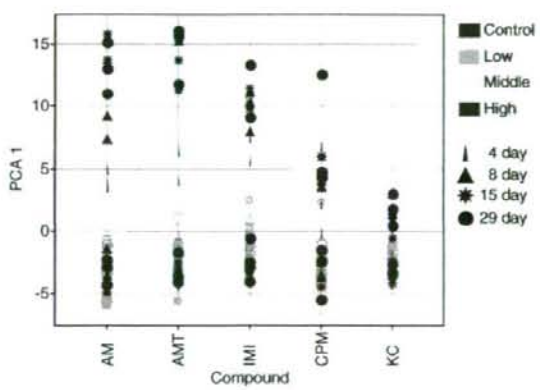

Fig. 3. Principal component analysis the same as Fig. 2 but with one dimensional expression using principal component 1. For each drug, each individual rat is depicted by a symbol with a different color and shape as shown on the right panel.

Discussion

PLsis has been one of the main concerns in the course of drug development, since its appropriate biomarkers are lacking, especially in the clinical field. In order to assess PLsis, a variety of in vitro methodologies have recently been described, e.g., using fluorescent dyes (Casartelli et al., 2003) or fluorescently labeled phospholipids (Kasahara et al., 2006, Nioi et al., 2007) in cell culture. However, these assay systems only work to estimate the potential of PLsis, but not to tell its mechanism and thus they do not help in deciding whether to go ahead or to switch to other candidates in the development process. One promising strategy would be a toxicogenomics approach. Sawada et al. (2005) recently identified a panel of 17 genes where the expression profile would predict the possibility of PLsis using HepG2 cells. This result was further transferred to a 96-well plate to attain a high throughput genomics-based platform (Sawada et al., 2006). Although the advantage of the genomics-based strategy was postulated to elucidate the background toxicological mechanism, the gene expression changes have not been related to the pathophysiological aspects of PLsis. It has been suggested that PLsis is induced by the disturbance of lipid turnover, i.e., excess of lipid biosynthesis, inhibition of lipid degradation enzymes (especially lysosomal phospholipase A2), and inhibition of lipid transporter in lysosomes. In the case of drug-induced PLsis, most of it has been attributed to the inhibition of phospholipase

Table 5
List of 28 probe sets contributing PC1

Ranking	Probe set ID	Gene title	Eigenvalue
1	1368905_at	Carboxylesterase 2 (intestine, liver)	0.165043
2	1387759_s_at	UDP glycosyltransferase 1 family, polypeptide A1	0.163056
3	1387022_at	Aldehyde dehydrogenase family 1, member A1	0.158847
4	1371076_at	Cytochrome P450, family 2, subfamily b, polypeptide 15	0.156238
5	1387118_at	Cytochrome P450, family 3, subfamily a, polypeptide 1	0.153634
6	1387109_at	P450 (cytochrome) oxidoreductase	0.152900
7	1371089_at	Transcribed locus	0.152322
8	1368718_at	Aldehyde dehydrogenase family 1, subfamily A4	0.147161
9	1370613_s_at	UDP glycosyltransferase 1 family, polypeptide A1	0.145621
10	1368977_a_at	Fractured callus expressed transcript 1	0.145613
11	1370583_s_at	ATP-binding cassette, subfamily B (MDR/TAP), member 1	0.145395
12	1380254_at	Transcribed locus, moderately similar to NP_079928.1 general transcription factor III A [*Mus musculus*]	0.145244
13	1387669_a_at	Epoxide hydrolase 1, microsomal	0.144549
14	1370698_at	Liver UDP-glucuronosyltransferase, phenobarbital-inducible form liver	0.143250
15	1368213_at	P450 (cytochrome) oxidoreductase	0.142376
16	1375423_at	MAX-like protein X	0.135972
17	1387094_at	Solute carrier organic anion transporter family, member 1a4	0.131073
18	1372602_at	Similar to genethonin 1	0.129514
19	1369850_at	UDP-glucuronosyltransferase 2 family, polypeptide A1	0.129217
20	1368275_at	Sterol-C4-methyl oxidase-like	0.129122
21	1371875_at	Mannosidase, beta A, lysosomal	0.128496
22	1372479_at	Transcribed locus, moderately similar to NP_064456.1 fibrinogen, beta polypeptide [*Rattus norvegicus*]	0.127711
23	1387093_at	Solute carrier organic anion transporter family, member 1a4	0.127266
24	1371809_at	Mitochondrial ribosomal protein S18B	0.126952
25	1384169_a_at	Vav2 oncogene (predicted)	0.125901
26	1375909_at	Similar to glutathione transferase GSTM7-7	0.125538
27	1373924_at	Similar to C530044N13Rik protein	0.122349
28	1371680_at	Similar to gamma-aminobutyric acid (GABA(A)) receptor-associated protein-like 1	0.117093

activity either through the generation of CAD-phospholipid complexes or by direct inhibition of phospholipase activity (Reasor et al., 2006). It is clearly necessary to elucidate how these changes are reflected in gene expression in order to make a prediction based on the genomics approach.

In the present study, we extracted 78 genes commonly mobilized in the 5 typical PLsis-inducing drugs, i.e., AM (Honegger et al., 1993), AMT (Drenckhahn et al., 1976), CPM (Xia et al., 2000), IMI (Drew et al., 1981; Hansson et al., 1997) and KC (Whitehouse et al., 1994). By PCA, we used these genes to successfully separate the high risk group from the low risk ones, except for KC, which showed relatively obscure separation. This is reasonable, as the histopathology of KC only causes changes

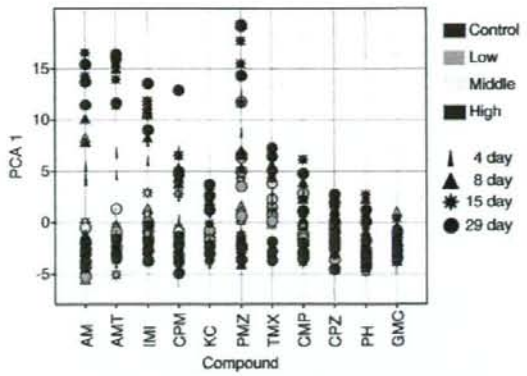

Fig. 4. Principal component analysis of gene expression profiles of 6 compounds reported to induce PLsis but no abnormality in present histopathological examination, i.e., chloramphenicol (CMP), chlorpromazine (CPZ), gentamicin (GMC), perhexiline (PH), promethazine (PMZ), and tamoxifen (TMX) using the commonly mobilized 78 probe sets. For comparison, 5 compounds shown in Figs. 2 and 3, amiodarone (AM), amitriptyline (AMT), clomipramine (CPM), imipramine (IMI), and ketoconazole (KC), are also included. Results are expressed as a one dimensional figure with PC1 (contribution rate: 34.8%). For each drug, each individual rat is depicted by a symbol with a different color and shape as shown on the right panel.

in the bile duct cells, in contrast to the other 4 drugs that elicit changes in the hepatocytes.

CMP (Joshi et al., 1989), CPZ (Kodavanti et al., 1990), GMC (Kacew, 1987), PH (Pessayre et al., 1979), PMZ (Joshi et al., 1989) and TMX (Reasor and Kacew, 2001) have also been reported to induce PLsis, but we could not detect PLsis in liver by histopathological examinations in the present study. This is not surprising when the sensitivity of detection by histopathology is

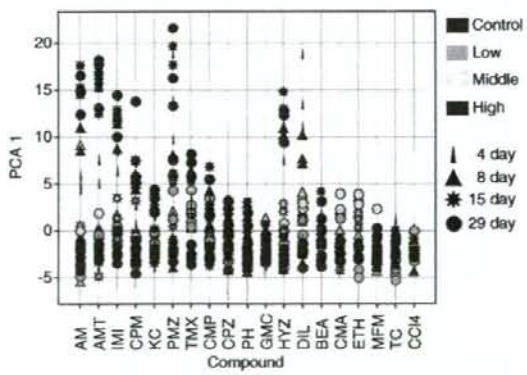

Fig. 5. Principal component analysis of gene expression profiles of 8 compounds showing pathological changes similar to PLsis, i.e., carbon tetrachloride (CCL4), coumarin (CMA), tetracycline (TC), metformin (MFM), hydroxyzine (HYZ), diltiazem (DIL), 2-bromoethylamine (BEA), and ethionamide (ETH), using the commonly mobilized 78 probe sets. For comparison, the 5 compounds shown in Figs. 2 and 3, amiodarone (AM), amitriptyline (AMT), clomipramine (CPM), imipramine (IMI) and ketoconazole (KC), and the 6 compounds in Fig. 4, chloramphenicol (CMP), chlorpromazine (CPZ), gentamicin (GMC), perhexiline (PH), promethazine (PMZ), and tamoxifen (TMX) are also included. Results are expressed as a one dimensional figure with PC1 (contribution rate: 34.8%). For each drug, each individual rat is depicted by a symbol with a different color and shape as shown on the right panel.

considered. In particular, our dose setting for the database was based on preliminary experiments of repeated dosing for 7 days with the proviso that all animals are to survive for 28 days. This sometimes brings about a situation that the dose level is too low for certain phenotypes. This point is particularly problematic when biomarker gene lists are to be extracted based on the actually observed phenotype. Of these 6 drugs, we could judge CMP, PMZ and TMX as positive by PCA using the present marker genes, whereas CPZ, GMC and PH were weakly positive or almost negative. These observations could be due to a feature of the marker genes: a considerable part of them actually reflects the occurring pathological changes, namely, they work as diagnostic markers. The fact that some of the drugs could be judged as positive suggested that their diagnosis from marker genes was more sensitive than pathological examination.

GMC has been reported to cause PLsis in kidney tissue and this is associated with renal tubular toxicity (Kaloyanides and Pastoriza-Munoz, 1980; Laurent et al., 1990). This might be attributed to its negative judgment for PLsis in liver since potential biochemical/pathological changes would mainly occur in kidney. It is of interest to investigate the gene expression changes in kidney, but another set of genes would be necessary to make a precise diagnosis for PLsis in kidney.

PH was selected as a PLsis-positive drug but appeared to be negative or a very weak positive in the present study using rats. This might be due to the species difference in the drug metabolism since the risk of PH-induced liver injury is higher in individuals with the P450IID6 poor-metabolizer phenotype (Morgan et al., 1984, Pessayre and Larrey, 1988).

Some compounds show morphological changes similar to PLsis. In our database, there are 8 such compounds, i.e., CCL4, CMA, TC, MFM, HYZ, DIL, BEA, and ETH. Of these, CCL4 (Weber et al., 2003), TC (Fréneaux et al., 1988), BEA (Thiele-

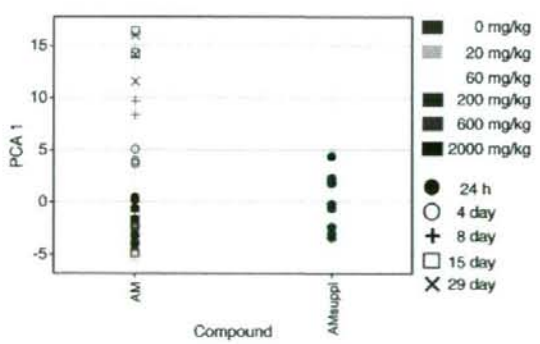

Fig. 6. Principal component analysis of gene expression profiles of amiodarone. Results are expressed as a one dimensional figure with PC1 (contribution rate: 34.8%). Each individual rat is depicted by a symbol with a different color and shape as shown on the right panel. On the left, the data of 24 h after a single treatment (filled symbols) are added to the data for repeated treatment (open or line symbols) shown in the previous figures. Note that the PC1 value of a single dose is low even at the highest dose, 200 mg/kg (red filled circle) compared with the repeated dose (red open or line symbols). On the left, a supplemental higher dose experiment was performed. Note that the higher dose (600 mg/kg, magenta; 2000 mg/kg, black) showed a dose-dependent increase in PC1 reaching to a value of 200 mg/kg at 4 days.

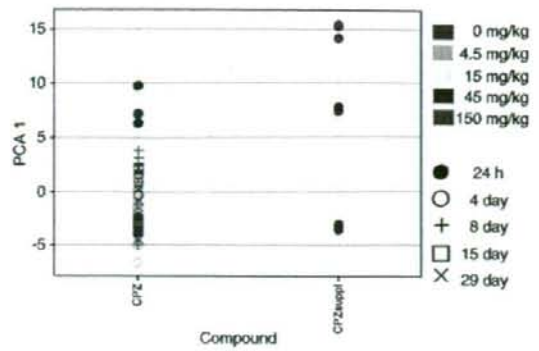

Fig. 7. Principal component analysis of gene expression profiles of chlorpromazine. Results are expressed as a one dimensional figure with PC1 (contribution rate: 34.8%). Each individual rat is depicted by a symbol with a different color and shape as shown on the right panel. On the left, the data of 24 h after a single treatment (filled symbols) are added to the data for repeated treatment (open or line symbols) shown in the previous figures. In contrast to the results in Fig. 6, the single dose of 45 mg/kg (red filled circle) gave higher PC1 values compared with samples of repeated dosing. On the left, a supplemental higher dose (150 mg/kg) experiment was performed in addition to 45 mg/kg. Note that the higher dose (magenta) showed even higher PC1 values.

mann et al., 1999), and ETH (Kuntz et al., 1968, Inouye et al., 1973) are reported to show morphology associated with a change in the lipid storage, i.e., lipidosis or steatosis. CMA is known to cause hepatic necrosis (Lake, 1984) and MFM induces a deposition of glycogen. These drugs, which do not induce PLsis, could be separated from the clusters of PLsis-inducing ones by PCA using the extracted genes. As for HYZ (Hruban et al., 1972), classified as PLsis-positive by PCA in this study, there is a recent report that it actually induced PLsis (Pelletier et al., 2007). The only exception was the case of DIL, which showed vacuolation in hepatocytes and was not considered as PLsis, but was classified as positive by PCA. Reviewing the PCA (Fig. 5) however, it is noticeable that the time-dependent changes in the PC1 value are exceptionally different from other drugs such that the value transiently increases with the peak at 4 days, then decreases with time and returns to negative at the 15th day. It is necessary to elucidate the mechanism of the unique change observed in DIL, but it appears that this drug is to be judged as pseudo-positive by the present criteria.

One important question is whether the toxicogenomics approach enables not only diagnosis but also prognosis of PLsis. The results shown in Figs. 6 and 7 provide a clue. In general, it appears to be difficult to predict the potential of PLsis occurring 14 days or later with repeated administration with the data for single dosing, but it could be possible when a high enough dose is applied in some cases. We are presently in a preliminary stage, but we hope to establish a really useful marker gene set in a future study with a strategic protocol, which can predict PLsis in liver by single dosing within 24 h. In the present study, we exclusively worked on liver where enough gene expression data are stored in our database. As PLsis occurs in organs other than liver, it is of interest to apply the present strategy to other organs such as kidney whose transcriptome data are now accumulating in our database.

There remain many problems to be solved in the present system, such as the improvement of accuracy and sensitivity, the elucidation of the functions of the genes in the list (especially in the pathological mechanism of PLsis), the breakthrough species difference, and so on. However, the presently identified 78 probe sets from gene expression data stored in TG-GATEs have provided a powerful starting tool.

Acknowledgment

This work was supported in part by the grants from Ministry of Health, Labour and Welfare of Japan, H14-001-Toxico.

References

Casartelli, A., Bonato, M., Cristofori, P., Crivellente, F., Dal Negro, G., Masotto, I., Mutinelli, C., Valko, K., Bonfante, V., 2003. A cell-based approach for the early assessment of the phospholipidogenic potential in pharmaceutical research and drug development. Cell Biol. Toxicol. 19, 161–176.

Dennis Jr., G., Sherman, B.T., Hosack, D.A., Yang, J., Gao, W., Lane, H.C., Lempicki, R.A., 2003. DAVID: database for annotation, visualization, and integrated discovery. Genome Biol. 4, P3.

Drenckhahn, D., Kleine, L., Lullmann-Rauch, R., 1976. Lysosomal alterations in cultured macrophages exposed to anorexigenic and psychotropic drugs. Lab. Invest. 35, 116–123.

Drew, R., Siddik, Z.H., Mimnaugh, E.G., Gram, T.E., 1981. Species and dose differences in the accumulation of imipramine by mammalian lungs. Drug Metab. Dispos. 9, 322–326.

Fréneaux, E., Labbe, G., Letteron, P., The Le Dinhi, Degott, C., Genève, J., Larrey, D., Pessayre, D., 1988. Inhibition of the mitochondrial oxidation of fatty acids by tetracycline in mice and in man: possible role in microvesicular steatosis induced by this antibiotic. Hepatology 8, 1056–1062.

Halliwell, W.H., 1997. Cationic amphiphilic drug-induced phospholipidosis. Toxicol. Pathol. 25, 53–60.

Hansson, A.L., Xia, Z., Berglund, M.C., Bergstrand, A., Depierre, J.W., Nässberger, L., 1997. Reduced cell survival and morphological alterations induced by three tricyclic antidepressants in human peripheral monocytes and lymphocytes and in cell lines derived from these cell types. Toxicol. In Vitro 11, 21–31.

Honegger, U.E., Zuehlke, R.D., Scuntaro, I., Schaefer, M.H., Toplak, H., Wiesmann, U.N., 1993. Cellular accumulation of amiodarone and desethylamiodarone in cultured human cells. Consequences of drug accumulation on cellular lipid metabolism and plasma membrane properties of chronically exposed cells. Biochem. Pharmacol. 45, 349–356.

Hruban, Z., Slesers, A., Hopkins, E., 1972. Drug-induced and naturally occurring myeloid bodies. Lab. Invest. 27, 62–70.

Inouye, B., Yoshimura, N., Wachi, T., 1973. Experimental studies on the mechanism of fatty liver formation induced by ethionamide. V. Liver and serum total cholesterol in ethionamide-administered rats. Kekkaku 48, 71–74.

Joshi, U.M., Rao, P., Kodavanti, S., Lockard, V.G., Mehendale, H.M., 1989. Fluorescence studies on binding of amphiphilic drugs to isolated lamellar bodies: relevance to phospholipidosis. Biochim. Biophys. Acta 1004, 309–320.

Kacew, S., 1987. Cationic amphiphilic drug-induced renal cortical lysosomal phospholipidosis: an in vivo comparative study with gentamicin and chlorphentermine. Toxicol. Appl. Pharmacol. 91, 469–746.

Kaloyanides, G.J., Pastoriza-Munoz, E., 1980. Aminoglycoside nephrotoxicity. Kidney Int, 18, 571–582.

Kasahara, T., Tomita, K., Murano, H., Harada, T., Tsubakimoto, K., Ogihara, T., Ohnishi, S., Kakinuma, C., 2006. Establishment of an in vitro high-throughput screening assay for detecting phospholipidosis-inducing potential. Toxicol. Sci. 90, 133–141.

Kodavanti, U.P., Lockard, V.G., Mehendale, H.M., 1990. In vivo toxicity and pulmonary effects of promazine and chlorpromazine in rats. J. Biochem. Toxicol. 5, 245–251.

Kuntz, E., Liehr, H., Pfingst, W., 1968. Toxic liver damage due to ethionamide. Ger. Med. Mon. 13, 599–602.

Lake, B.G., 1984. Investigations into the mechanism of coumarin-induced hepatotoxicity in the rat. Arch. Toxicol. Suppl. 7, 16–29.

Laurent, G., Kishore, B.K., Tulkens, P.M., 1990. Aminoglycoside-induced renal phospholipidosis and nephrotoxicity. Biochem. Pharmacol. 40, 2383–2392.

Morgan, M.Y., Reshef, R., Shah, R.R., Oates, N.S., Smith, R.L., Sherlock, S., 1984. Impaired oxidation of debrisoquine in patients with perhexiline liver injury. Gut 25, 1057–1064.

Nioi, P., Perry, B.K., Wang, E.J., Gu, Y.Z., Snyder, R.D., 2007. In vitro detection of drug-induced phospholipidosis using gene expression and fluorescent phospholipid based methodologies. Toxicol. Sci. 99, 162–173.

Pelletier, D.J., Gehlhaar, D., Tilloy-Ellul, A., Johnson, T.O., Greene, N., 2007. Evaluation of a published in silico model and construction of a novel bayesian model for predicting phospholipidosis inducing potential. J. Chem. Inf. Model 47, 1196–1205.

Pessayre, D., Bichara, M., Degott, C., Potet, F., Benhamou, J.P., Feldmann, G., 1979. Perhexiline maleate-induced cirrhosis. Gastroenterol. 76, 170–177.

Pessayre, D., Larrey, D., 1988. Acute and chronic drug-induced hepatitis. Baillieres Clin. Gastroenterol. 2, 385–422.

Reasor, M.J., Kacew, S., 2001. Drug-induced phospholipidosis: are there functional consequences? Exp. Biol. Med. 226, 825–830.

Reasor, M.J., Hastings, K.L., Ulrich, R.G., 2006. Drug-induced phospholipidosis: issues and future directions. Expert Opin. Drug Saf. 5, 567–583.

Sawada, H., Takami, K., Asahi, S., 2005. A toxicogenomic approach to drug-induced phospholipidosis: analysis of its induction mechanism and establishment of a novel in vitro screening system. Toxicol. Sci. 83, 282–292.

Sawada, H., Taniguchi, K., Takami, K., 2006. Improved toxicogenomic screening for drug-induced phospholipidosis using a multiplexed quantitative gene expression ArrayPlate assay. Toxicol. In Vitro 20, 1506–1513.

Takashima, K., Mizukawa, Y., Morishita, K., Okuyama, M., Kasahara, T., Toritsuka, N., Miyagishima, T., Nagao, T., Urushidani, T., 2006. Effect of the difference in vehicles on gene expression in the rat liver-analysis of the control data in the Toxicogenomics Project Database. Life Sci. 78, 2787–2796.

Thielemann, L.E., Bosco, C., Rodrigo, R., Orellana, M., Videla, L.A., 1999. Effects of bromoethylamine on antioxidant capacity, lipid peroxidation, and morphological characteristics of rat liver. J. Biochem. Mol. Toxicol. 13, 47–52.

Tomizawa, K., Sugano, K., Yamada, H., Horii, I., 2006. Physicochemical and cell-based approach for early screening of phospholipidosis-inducing potential. J. Toxicol. Sci. 31, 315–324.

Urushidani, T., Nagao, T., 2005. Toxicogenomics: the Japanese initiative. In: Borlak, J. (Ed.), Handbook of Toxicogenomics—Strategies and Applications. Wiley-VCH, pp. 623–631.

Weber, L.W., Boll, M., Stampfl, A., 2003. Hepatotoxicity and mechanism of action of haloalkanes: carbon tetrachloride as a toxicological model. Crit. Rev. Toxicol. 33, 105–136.

Whitehouse, L.W., Menzies, A., Mueller, R., Pontefract, R., 1994. Ketoconazole-induced hepatic phospholipidosis in the mouse and its association with de-*N*-acetyl ketoconazole. Toxicology 94, 81–95.

Xia, Z., Ying, G., Hansson, A.L., Karlsson, H., Xie, Y., Bergstrand, A., DePierre, J.W., Nassberger, L., 2000. Antidepressant-induced lipidosis with special reference to tricyclic compounds. Prog. Neurobiol. 60, 501–512.

0090-9556/08/3609-1786–1793$20.00
DRUG METABOLISM AND DISPOSITION
Copyright © 2008 by The American Society for Pharmacology and Experimental Therapeutics
DMD 36:1786–1793, 2008

Vol. 36, No. 9
20073/3370086
Printed in U.S.A.

Decreased Expression of Cytochromes P450 1A2, 2E1, and 3A4 and Drug Transporters Na^+-Taurocholate-Cotransporting Polypeptide, Organic Cation Transporter 1, and Organic Anion-Transporting Peptide-C Correlates with the Progression of Liver Fibrosis in Chronic Hepatitis C Patients

Kenya Nakai, Hiromasa Tanaka, Kazuhiko Hanada, Hiroyasu Ogata, Fumitaka Suzuki, Hiromitsu Kumada, Atsuko Miyajima, Seiichi Ishida, Momoko Sunouchi, Wataru Habano, Yuichiro Kamikawa, Keiichi Kubota, Junji Kita, Shogo Ozawa, and Yasuo Ohno

Division of Pharmacology (K.N., H.T., A.M., S.I., M.S., S.O.) and Deputy Director General (Y.O.), National Institute of Health Sciences, Kamiyoga, Setagaya-ku, Tokyo, Japan; Department of Biopharmaceutics, Meiji Pharmaceutical University, Noshio, Kiyose, Tokyo, Japan (K.N., H.T., K.H., H.O.); Department of Hepatology, Toranomon Hospital, Toranomon, Minato-ku, Tokyo, Japan (F.S., H.K.); Department of Pharmacodynamics and Molecular Genetics, Faculty of Pharmaceutical Sciences, Iwate Medical University, Nishitokuta, Yahabacho, Shiwa-gun, Iwate, Japan (W.H., S.O.); Department of Pharmacology and Surgery Division (Y.K.) and Second Department of Surgery (K.K., J.K.), Dokkyo Medical University School of Medicine, Mibu, Tochigi, Japan

Received December 18, 2007; accepted May 29, 2008

ABSTRACT:

Patients with chronic hepatitis C viral infection underwent liver biopsies and laboratory studies for evaluation and to determine subsequent treatment. Changes in status of drug metabolism and disposition may vary with chronic hepatitis C stage and should be assessed. Total RNA was extracted from liver biopsy specimens (n = 63) and reverse transcribed to yield cDNA. Relative mRNA levels of drug-metabolizing enzymes, transporters, nuclear receptors, and proinflammatory cytokines were analyzed with normalization to glyceraldehyde 3-phosphate dehydrogenase expression. mRNAs encoding cytochromes P450 1A2, 2E1, and 3A4, and drug transporters, Na^+-taurocholate-cotransporting polypeptide, organic anion-transporting peptide-C, and organic cation transporter 1 showed remarkable decreases, and tumor necrosis factor-α showed an increase according to fibrosis stage progression. HepG2 cells and primary hepatocytes of two human individuals were treated with interleukin 1β, interleukin 6, or tumor necrosis factor-α. CYP1A2 and Na^+-taurocholate-cotransporting polypeptide mRNA levels significantly decreased in HepG2 cells with interleukin 1β and interleukin 6 treatments. CYP2E1 and organic cation transporter 1 mRNA levels significantly decreased with tumor necrosis factor-α treatment only in HepG2. These results suggested that down-regulation of CYP1A2, 2E1, and 3A4, and drug transporters, Na^+-taurocholate-cotransporting polypeptide, organic anion-transporting peptide-C, and organic cation transporter 1, manifested in livers of patients with chronic hepatitis C viral infection, was associated, at least in part, with the elevated production of proinflammatory cytokines, including tumor necrosis factor-α.

Infection and inflammation generally cause a decrease in hepatic capacity for drug metabolism and disposition. Using lipopolysaccharide models of hepatic inflammation, a number of investigators have demonstrated decreases in the expression of various drug-metabolizing enzymes (Iber et al., 1999; Renton, 2004). Bacterial and viral infections are associated with the induction of various cytokines, including interleukins (ILs) 1β and 6, tumor necrosis factor (TNF)-α, and interferon-γ, which decrease the level of hepatic drug-metabolizing enzymes (Iber et al., 1999; Renton, 2004). Hepatitis C virus (HCV) infection was reported to cause changes in levels of drug-metabolizing enzymes cytochrome P450 2E1 (Gochee et al., 2003), an oxidative stress-related enzyme, and glutathione peroxidase (Levent et al., 2006); and nuclear receptors, including peroxisome proliferator-

This study was supported in part by a grant from the Human Science Foundation of Japan, by a Grant-in-Aid from the Ministry of Health, Labor and Welfare, Japan, and by a Grant-in-Aid from the Japanese Ministry of Education, Science and Culture.

Article, publication date, and citation information can be found at http://dmd.aspetjournals.org.

doi:10.1124/dmd.107.020073.

ABBREVIATIONS: IL, interleukin; TNF, tumor necrosis factor; HCV, hepatitis C virus; ROS, reactive oxygen species; PCR, polymerase chain reaction; NTCP, Na^+-taurocholate-cotransporting peptide; OATP-C, organic anion-transporting peptide-C; OCT1, organic cation transporter 1; MRP, multidrug resistance-associated protein; MDR, multidrug resistance protein; CAR, constitutive androstane receptor; SULT, sulfotransferase; HNF, hepatocyte nuclear factor; GAPDH, glyceraldehyde-3-phosphate dehydrogenase; ANOVA, analysis of variance; INR, international normalized ratio.

TABLE 1

Histopathological features and demographics in chronic hepatitis C infection

No subject received interferon therapy before liver biopsy.

	Patients with Chronic Hepatitis C (n = 63)
Age (years)	53 ± 10
Sex (male/female)	34/29
Smoking (n)	20
Alcohol (n)	21
Major medications	
Glycyrrhizic acid/ursodeoxycholic acid	F_1 (6), F_2 (2), F_3 (4)
Amlodipine/nicardipine/atenolol	F_1 (5), F_2 (2), F_3 (2)
Brotizolam/alprazolam/triazolam	F_1 (4), F_2 (1), F_3 (0)
Glimepiride/nateglinide	F_1 (4), F_2 (1), F_3 (1)
Pathological class	
Fibrosis staging (n)	F_0 (0), F_1 (35), F_2 (11), F_3 (17), F_4 (0)
Inflammation grading (n)	A_0 (0), A_1 (38), A_2 (25), A_3 (0)

activated receptor-α (Dharancy et al., 2005). Immune-mediated liver damage, viral product-mediated cytotoxicity, and oxidative stress have also been documented to play a role in the pathogenicity of HCV infection. Production of cytokines, such as TNF-α, which is associated with the generation of reactive oxygen species (ROS), is increased in patients with chronic hepatitis C, causing oxidative stress in these patients (Choi et al., 2004). Despite much accumulated knowledge of the pathophysiology of various infectious diseases, including HCV, there is little information on liver-specific markers that indicate individual drug elimination capacities during HCV infection. In this report, we describe the results of a comprehensive study of variations of mRNA levels of drug-metabolizing enzymes and drug transporters in chronic hepatitis C patients. Using quantitative real-time polymerase chain reaction (PCR) analysis, liver biopsy samples from 63 Japanese patients were examined. We observed clear correlations between fibrosis stage and mRNA levels of hepatic CYP1A2, CYP2E1, and CYP3A4, and the drug transporters Na^+-taurocholate-cotransporting peptide (NTCP), organic anion-transporting peptide-C (OATP-C), and organic cation transporter 1 (OCT1). A fibrosis stage-dependent increase in TNF-α mRNA level was observed in our study population. mRNAs involved in drug metabolism and disposition were also examined in relationship to clinical laboratory data on hepatic and renal function. In addition, exposure of a human hepatoblastoma cell line, HepG2, and human primary hepatocytes of two human individuals to TNF-α partly resulted in a decrease in CYP2E1 mRNA activity and OCT1 mRNA levels. Exposure of HepG2 cells to IL-1 and IL-6 resulted in a decrease in CYP1A2 and NTCP mRNA levels. The data provide information on fibrosis stage-associated changes in gene expression related to hepatic drug metabolism and disposition, which is useful for drug therapy for patients with chronic hepatitis C infection.

Materials and Methods

Subjects. Ultrasound-guided or laparoscopic liver biopsy was performed on 63 patients with chronic hepatitis C at Toranomon Hospital, Tokyo, Japan. Fibrosis staging was divided into four classes: F_0, no fibrosis; F_1, periportal expansion; F_2, portoportal septa; and F_3, portocentral linkage or bridging fibrosis (Desmet et al., 1994). No patients with liver cirrhosis (F_4) were included in this study. Inflammatory activity was divided into four classes: A_0, no necroinflammatory reaction; A_1, mild necroinflammatory reaction; and A_2, moderate necroinflammatory reaction (Desmet et al., 1994). No A_3 patients with severe necroinflammatory reaction were included in this study (Table 1). Eight liver biopsy samples were excluded because of degraded RNA. RNA quality was evaluated using an Agilent 2100 Bioanalyzer (Agilent Technologies, Palo Alto, CA) (Fig. 1). Clinical laboratory data were collected (Table 2) from patients who were evaluated on the same or previous day that the liver biopsy was performed. Clinical data and history were obtained from each patient's chart, which was stored at Toranomon Hospital. Noncancerous liver tissues, which were resected at the Dokkyo Medical University School of Medicine from 21 patients (13 males and eight females, 39–82 years old) with metastatic liver cancer originated from colon cancer, were also used. We obtained three noncancerous liver samples taken from patients (two males and one female, 61 to 71 years old) with metastatic liver cancer originated from colon through the Health Science Research Resources Bank (Osaka, Japan). These donor patients were free from both chronic hepatitis B and C viruses. RNA quality was also evaluated using an Agilent 2100 Bioanalyzer (Agilent Technologies). The study protocol was approved by an independent ethics committee from Toranomon Hospital, Dokkyo Medical University School of Medicine, the National Institute of Health Sciences, and Meiji Pharmaceutical University, and conformed to the 1975 Declaration of Helsinki ethical guidelines. Written informed consent was obtained from all patients participating in the study.

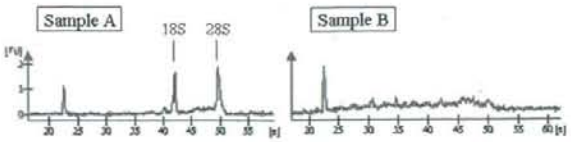

FIG. 1. Analysis for RNA degradation by the Agilent 2100 Bioanalyzer. Total RNA extracted from 63 Japanese patients was subjected to electrophoretic analysis. As shown in sample A, 28S and 18S rRNAs were detected as sharp peaks, whereas in sample B, both rRNAs sizes were completely degraded. Of the 63 samples, eight samples showed a high degree of RNA degradation and therefore were excluded from subsequent analyses.

TABLE 2

Chronic hepatitis C patient laboratory data

Clinical Laboratory Data	Number or Value (Mean ± S.D.; Range)
Viral load (KIU/ml)	777 ± 596
HCV genotype	
1a	1
1b	42
2a	13
2b	7
ALT (IU/l)	139 ± 93; 36–414
AST (IU/l)	88 ± 53; 23–276
γ-GTP (IU/l)	89 ± 73; 17–264
ALP (IU/l)	218 ± 78; 81–430
LDH (IU/l)	159 ± 27; 104–256
Total bilirubin (mg/dl)	0.9 ± 0.3; 0.4–2.2
Total cholesterol (mg/dl)	165 ± 27; 109–222
Serum triglycerides (mg/dl)	99 ± 34; 38–183
HDL (mg/dl)	44 ± 11; 26–77
Cholinesterase (Δ pH assay)	1.1 ± 0.3; 0.6–2.1
Total protein (g/dl)	7.7 ± 0.6; 6.5–9.4
Prothrombin time (INR)	1.05 ± 0.09; 0.86–1.34
AFP (ng/ml)	16.2 ± 36.3; 2–256
Fe (μg/dl)	168.1 ± 58.4; 20–256
UIBC (μg/dl)	184.3 ± 84.2; 18–449
Ferritin (ng/ml)	240 ± 286; 12–1378
Hyaluronic acid (μg/l)	104.6 ± 117; 15–589

ALT, alanine aminotransferase; AST, aspartate aminotransferase; γ-GTP, γ-glutamyl transpeptidase; ALP, alkaline phosphatase; LDH, lactate dehydrogenase; HDL, high density lipoprotein; AFP, α-fetoprotein; UIBC, unsaturated iron binding capacity.

RNA Extraction, Reverse Transcription, and Real-Time PCR. The analyzed liver tissues of chronic hepatitis C patients weighed 1 to 25 mg (mean ± S.D. = 5.9 ± 5.4 mg), weight of nonhepatitis C patients ranged from 50 to 750 mg, and samples were stored at −70°C until used. The liver specimens were homogenized three times for 15 s in Lysis/Binding Solution from an RNA isolation kit (RNAqueous; Ambion, Austin, TX), using a Kinematica Polytron homogenizer (PT10–35; Kinematika, Lucerne, Switzerland). Total RNA (200 ng) was reverse transcribed to yield cDNA using TaqMan Reverse Transcription Reagents (Applied Biosystems, Foster City, CA). Real-time PCR was performed with probe and primer sets (TaqMan Gene Expression Assays) available from Applied Biosystems using an ABI PRISM

TABLE 3

Probe and primer sets (TaqMan Gene Expression Assays) used in this study

Gene Symbol	Alias	Assay Identification	RefSeq or GenBank Accession No.	Exon Boundary	Amplicon Length
					bp
CYP1A2	CYP1A2	Hs00167927_m1	NM_000761.3	2–3	67
CYP2A6	CYP2A6	Hs00868409_s1	NM_000762.4	9–9	131
CYP2B6	CYP2B6	Hs00167937_g1	NM_000767.4	7–8	88
CYP2C8	CYP2C8	Hs00258314_m1	M17398.1	7–8	108
CYP2C9	CYP2C9	Hs00426397_m1	NM_000771.2	6–7	148
CYP2C19	CYP2C19	Hs00426380_m1	NM_000769.1	5–6	106
CYP2D6	CYP2D6	Hs00164385_m1	NM_000106.4	2–3	74
CYP2E1	CYP2E1	Hs00559368_m1	NM_000773.3	6–7	74
CYP3A4	CYP3A4	Hs00604506_m1	NM_017460.3	2–3	119
CYP3A5	CYP3A5	Hs00241417_m1	NM_000777.2	3–4	82
ABCC1	MRP1	Hs00219905_m1	NM_004996.2	24–25	74
ABCC2	MRP2	Hs00166123_m1	NM_000392.1	25–26	75
ABCC3	MRP3	Hs00358656_m1	NM_003786.2	8–9	98
ABCB1	MDR1	Hs00184500_m1	NM_000927.3	6–7	67
ABCC4	MDR3	Hs00251620_m1	BC042531.1	25–26	69
SLC10A1	NTCP	Hs00161820_m1	NM_003049.1	1–2	68
SLCO1A2	OATP-A	Hs00366488_m1	NM_134431.1	13–14	72
SLCO2B1	OATP-B	Hs00200670_m1	NM_007256.2	7–8	113
SLCO1B1	OATP-C	Hs00272374_m1	NM_006446.2	14–15	77
ABCB11	BSEP	Hs00184824_m1	NM_003742.2	21–22	63
ABCG2	BCRP	Hs00184979_m1	NM_004827.2	5–6	92
SLC22A1	OCT1	Hs00427554_m1	NM_003057.2	8–9	66
SLC22A7	OAT2	Hs00198527_m1	NM_153320.2	5–6	69
NR1I3	CAR	Hs00231959_m1	NM_005122.2	8–9	84
NR1I2	PXR	Hs00243666_m1	NM_033013.1	5–6	68
VDR	NR1I1	Hs00172113_m1	NM_001017535.1	3–4	62
UGT1A1	UGT1A1	Hs01589938_m1	NM_000463.1	1–1	134
PPARA	PPARα	Hs00231882_m1	NM_001001928.2	3–4	147
SULT2A1	HST	Hs00234219_m1	NM_003167.2	4–5	98
SULT2B1	HSST2	Hs00190268_m1	NM_177973.1	2–3	80
HNF4A	HNF4α	Hs00230853_m1	NM_178849.1	3–4	49
PCBD2	DCOHM[a]	Hs00259792_m1	NM_032151.3	1–2	126
IL1B	IL-1β	Hs00174097_m1	NM_000576.2	5–6	94
IL6	IL-6	Hs00985639_m1	NM_000600.2	2–3	66
TNF	TNF-α	Hs00174128_m1	NM_000594.2	3–4	80

[a] Dimerization cofactor of HNF1α (TCF1) 2.

7700 Sequence Detection System (Applied Biosystems) for the quantitative analysis of mRNA encoding the following drug metabolism enzymes, drug transporters, nuclear receptors, and proinflammatory cytokines: CYP1A2, 2A6, 2B6, 2C8, 2C9, 2C19, 2D6, 2E1, 3A4, and 3A5; multidrug resistance-associated proteins (MRPs) MRP1, MRP2, and MRP3; multidrug resistance proteins (MDRs) MDR1 and MDR3; NTCP; OATP-A, OATP-B, and OATP-C; bile salt export pump; breast cancer resistance protein; OCT1; organic anion transporter 2; constitutive androstane receptor (CAR); pregnane X receptor; vitamin D receptor; UDP glucuronosyltransferase 1A1; peroxisome proliferator-activated receptor-α; sulfotransferases (SULTs) SULT2A1 and SULT2B1; and hepatocyte nuclear factor (HNF) HNF4α and HNF1α dimerization cofactor; and IL-1β, IL-6, and TNF-α (Table 3). mRNA levels were normalized to glyceraldehyde-3-phosphate dehydrogenase (GAPDH). The ABI PRISM 7700 Sequence Detection System automatically created a standard curve by plotting the threshold cycle values against each standard dilution of a known standard human liver poly $(A)^+$ RNA concentration (BD Biosciences, San Jose, CA). Amounts of poly $(A)^+$ RNA used as a calibration standard that contained the same amounts of transcripts of interest (drug-metabolizing enzyme and so on) in the certain amount (200 ng) of patients' total RNAs were calculated and were given as A. The same procedure was performed for amounts of poly $(A)^+$ RNA that contained the same amounts of GAPDH transcripts in 200 ng of patients' total RNAs and were given as B. Relative mRNA levels were calculated as A/B, which were shown throughout in the present study and were compared among various liver samples. In principle, A is dependent on the mRNA copy numbers contained in the poly $(A)^+$ RNA used as a calibration standard. Therefore, comparison of A/B cannot be made between different genes. In our preliminary experiments, GAPDH and β-actin mRNA levels well correlated ($r = 0.7975$, $p < 0.001$), indicating that using GAPDH and β-actin gave quite similar results. We decided to use GAPDH for normalization, although justification of GAPDH usage has not fully been verified. All amplification reactions were carried out in duplicate. All mRNA level measurements were performed in at least two separate experiments, which had deviations within 7% of the mean values.

mRNA Levels for Genes Involved in Drug Metabolism and Disposition in HepG2 Cells and Primary Human Hepatocytes Treated with IL-1β, IL-6, or TNF-α. HepG2 cells, a human hepatoblastoma cell line, which were routinely cultured in Dulbecco's modified Eagle's medium supplemented with 10% fetal bovine serum, were treated with recombinant IL-1β (4 ng/ml; PeproTech EC, Rocky Hill, NJ), recombinant IL-6 (50 ng/ml; PeproTech EC), or recombinant TNF-α (0.25 ng/ml; Upstate, Lake Placid, NY) at 37°C for 24 h. These cytokine concentrations did not show any cytotoxicity for up to 72 h. The cells were washed twice with 5 ml of phosphate-buffered saline, pH 7.4, after cytokine exposure, and total RNA was purified using the RNeasy Mini Kit (QIAGEN GmbH, Hilden, Germany) according to the manufacturer's instructions. Two different human primary hepatocyte monolayers [human long-term hepatocytes in monolayer derived from a 73-year-old female (hepatocyte no. 1) and a 72-year-old male (hepatocyte no. 2)] were purchased through KAC Co. (Kyoto, Japan) from Biopredic (Renne, France). They were provided in a 24-well plate. The medium was replaced with long-term culture medium as indicated by the manufacturer and cultured for 2 days at 37°C. Then, the cells were treated with recombinant IL-1β (4 ng/ml; PeproTech EC), recombinant IL-6 (50 ng/ml; PeproTech EC), or recombinant TNF-α (0.25 ng/ml; Upstate) at 37°C for 24 h. Total RNAs were purified using the RNeasy Mini Kit (QIAGEN GmbH), as in the case of HepG2 cells. Total RNA was then reverse-transcribed by the High Capacity cDNA Reverse Transcription Kit (Applied Biosystems) and subjected to real-time PCR analyses for levels of CYP1A2, CYP2E1, CYP3A4, NTCP, OATP-C, and OCT1 mRNA by TaqMan Gene Expression Assay using an Applied Biosystems 7500 Real-time PCR system (Applied Biosystems). The RNA levels were normalized to GAPDH. The relative mRNA levels were determined in triplicate for HepG2 experi-

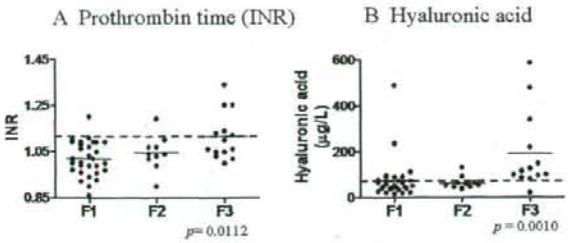

FIG. 2. Relationships between disease progression (fibrosis) and prothrombin time (INR) (A) and hyaluronic acid level (B). Clinical laboratory data were plotted in relationship to fibrosis stage. Black lines, means for each category. Red lines, highest limit of normal values. The statistical significance of the differences in the values between fibrosis stages was evaluated by the Kruskal-Wallis test and shown as p values.

ments. The results were expressed as mean ± S.D. Data are expressed as mean ± S.D. in four separate human hepatocyte experiments.

Measurement of CYP2E1 Activity. CYP2E1 activity in human primary hepatocytes was determined according to the method by Ito et al. (2007). In brief, cultured primary hepatocytes were incubated in a fresh media with 0.5 mM p-nitrophenol at 37°C for 60 min. The supernatant was assayed for 4-nitrocatechol by the addition of 10 M NaOH (1:10) and immediate determination of the absorbance at 546 nm. Activity after cytokine exposure was compared with that of control.

Determination of Viral Load. HCV RNA viral load in serum samples was calculated by the Amplicor quantification method (Amplicor HCV Monitor assay version 2.0; Roche Diagnostics, Tokyo, Japan).

Statistical Analysis. Statistical analysis was performed using the Kruskal-Wallis test, one-way analysis of variance (ANOVA) with a post hoc test (Tukey's multiple comparison test), the Mann-Whitney test, χ^2 test, and the Spearman rank correlation using GraphPad Prism version 4.02 (GraphPad Software Inc., San Diego, CA). In each test, $p < 0.05$ was considered statistically significant.

Results

Patient Characteristics. Table 1 describes the histopathological features of the liver samples, together with the age, sex, and smoking, drinking habits, and major medications of the chronic hepatitis C patients recruited in the present study. Liver biopsy was performed to decide subsequent therapy. Therefore, no patient received interferon before liver biopsy. There were 34 males, 29 females, and 20 smokers. There were no heavy drinkers, although 21 reported alcohol consumption. The patient distribution by fibrosis stages was: F_1, 35; F_2, 11; and F_3, 17. The distribution of inflammatory activity was: A_1, 38; and A_2, 25. The laboratory data from chronic hepatitis C patients are shown in Table 2. The mean HCV RNA viral load was 777 ± 596 KIU/ml, and HCV genotypes were divided into four classes (n): 1a (1), 1b (42), 2a (13), and 2b (7). Most of the Japanese chronic hepatitis C patients were infected with genotype 1b viruses, and the genotype 1b patients had high HCV RNA viral loads. The prothrombin times [international normalized ratio (INR)] and hyaluronic acid levels were significantly higher in F_3 patients than in F_2 patients (Fig. 2). Most of the F_3 patients had hyaluronic acid levels that were greater than the highest normal values (Fig. 2B). No correlation was observed between viral load and fibrosis stage, which was consistent with a previous report (Grønbaek et al., 2005).

Relationships among Relative mRNA Expression for Cytochromes P450, Drug Transporters, and Nuclear Receptors and Fibrosis Staging and Inflammation Grading in Chronic Hepatitis C Patients. We analyzed trends in mRNA expression of drug-metabolizing enzymes, drug transporters, nuclear receptors, and proinflammatory cytokines according to the progression of chronic hepatitis C measured by histological staging and grading. Samples of 55 of 63 chronic hepatitis C patients (eight samples were excluded because of RNA degradation, Fig. 1) were evaluated by a pathologist from F_1 to F_3: F_1, 31; F_2, 10; and F_3, 14; and from A_1 to A2, A_1, 34; and A_2, 21. mRNA levels of drug-metabolizing enzymes [CYP1A2 (Fig. 3A), CYP2E1 (Fig. 3B), and CYP3A4 (Fig. 3C)], and drug transporters, NTCP (Fig. 3D), OATP-C (Fig. 3E), and OCT1 (Fig. 3F), showed remarkable decreases as the fibrosis stage progressed. These parameters failed to correlate with increased inflammation, except for CYP1A2. The relative CYP1A2 mRNA levels showed marginal statistical significance with increased inflammation (plot not shown, $p = 0.0369$ by nonparametric Mann-Whitney test). No fibrosis stage-dependent differences were observed for all other genes studied (see *Materials and Methods*). For example, mRNA levels for CYP2D6 and MDR1 did not correlate (plots not shown, $p = 0.7059$ and $p = 0.9932$, respectively). For reference, mRNA levels for CYP1A2, CYP2E1, CYP3A4, NTCP, OATP-C, and OCT1 in the noncancerous and nonhepatitis C liver tissues from 24 human individuals, who suffered from colon cancer and underwent resection of liver metastasis, were used. In the case of CYP3A4 and OATP-C, mean mRNA levels of the nonhepatitis C livers were higher than those of F_1 patients, but not in regard to the other four mRNAs. Although determinations of mRNA levels of interest were performed in the same way after checking the quality of RNAs as in hepatitis C cases, the nonhepatitis C livers were derived from tissues surrounding tumors, not from healthy subjects. Therefore, some mRNAs may be down-regulated in the liver tissues surrounding cancerous tissues as in the case of hepatitis C patients. Alternatively, CYP1A2, CYP2E1, NTCP, and OCT1 might be once up-regulated in the initial F_1 stage after hepatitis C viral infection; thereafter, their expression levels gradually decrease to those in the non-HCV patients. One-way ANOVA analyses of these gene expressions indeed revealed statistically significant elevation of CYP1A2 ($p < 0.01$), CYP2E1 ($p < 0.01$), NTCP ($p < 0.01$), and OCT1 ($p < 0.05$) mRNA levels in the patients of the F_1 stage as compared with those in the non-HCV patients. Those in the F_3 patients were not statistically different from those in the non-HCV patients. This hypothesis should be clarified by further studies performed using liver samples obtained in one hospital. mRNA levels of TNF-α, but not those of IL-1β, increased with statistical significance as the fibrosis stage progressed. As illustrated in Fig. 4, TNF-α mRNA levels in F_3 patients were significantly higher than those of F_1 patients (one-way ANOVA, $p < 0.05$). IL-6 mRNA levels were too low to evaluate in relation to fibrosis stage: IL-6 was detected in two of 31 subjects with F_1 stage, one in 10 (F_2), and four in 14 (F_3) (χ^2 test, $p > 0.05$).

Expression of CYP1A2, CYP2E1, CYP3A4, NTCP, OATP-C, and OCT1 mRNAs in HepG2 Cells and Primary Human Hepatocytes Treated with Proinflammatory Cytokines. HepG2 cells were exposed to 4 ng/ml recombinant IL-1β, 50 ng/ml recombinant IL-6, or 0.25 ng/ml recombinant TNF-α at 37°C for 24 h, all of which did not show any appreciable cytotoxicity. mRNA levels of CYP1A2, CYP2E1, CYP3A4, NTCP, OATP-C, and OCT1 decreased as the fibrosis stage progressed and were measured after 24 h of cytokine exposure using real-time PCR as described under *Materials and Methods*. As shown in Fig. 5, CYP1A2 and NTCP mRNA levels were significantly decreased by IL-1β and IL-6 (by 26.1 and 37.1% for CYP1A2 and 89.6 and 96.4% for NTCP, respectively). CYP2E1 and OCT1 mRNA levels were significantly decreased by TNF-α treatment by 50.4 and 35.5%, respectively. IL-6 showed a tendency to decrease CYP2E1, CYP3A4, and OCT1 mRNA levels, which did not, however, reach statistical significance. No remarkable alteration of OATP-C mRNA was observed by exposure to IL-1β, IL-6, or TNF-α. Human primary hepatocytes of two different individuals were treated

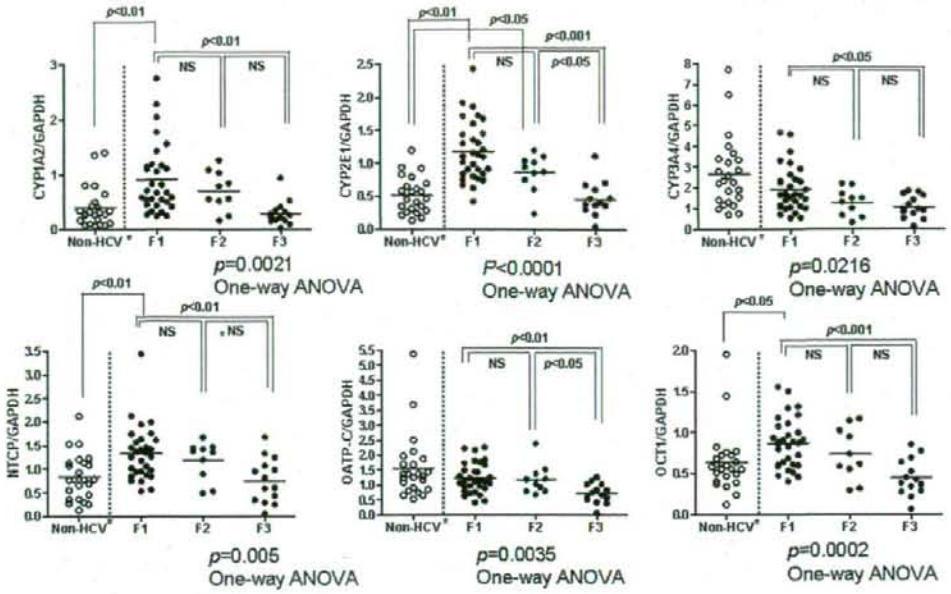

*Non-HCV livers were derived from non-cancerous liver tissues from individuals, who suffered from metastatic liver cancer originated from colon cancer.

FIG. 3. Reduced expression of CYP1A2 (upper left), CYP2E1 (upper middle), CYP3A4 (upper right), NTCP (lower left), OATP-C (lower middle), and OCT1 (lower right) in relationship to the progression of liver fibrosis in chronic hepatitis C patients. Relative mRNA levels for drug metabolism and disposition genes in 55 biopsy liver samples are plotted (closed circles) according to the disease stage defined by liver fibrosis. The methods for the determination of the relative mRNA levels are described under *Materials and Methods*. Degrees of statistical significance were analyzed by one-way ANOVA with a post hoc test (Tukey's multiple comparison test). N.S., not significant ($p > 0.05$). For reference, relative mRNA levels involved in drug metabolism and disposition in 24 liver noncancerous samples derived from human individuals, who underwent resection of metastatic liver cancer (originated from colon cancer) are plotted (open circles). Degrees of statistical significance were analyzed by one-way ANOVA with a post hoc test (Dunnet's multiple comparison test) throughout non-HCV and F_1 to F_3 HCV patients. Means of CYP1A2, CYP2E1, NTCP, and OCT1 were significantly different ($p < 0.001$). Statistical significance between values of non-HCV and each of F_1 to F_3 patients is shown on the graph in the case of significant difference.

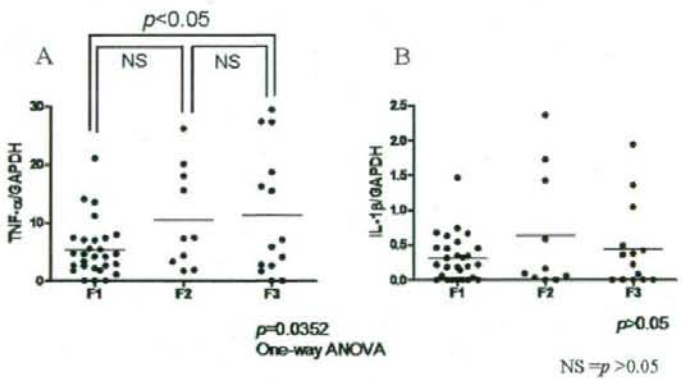

FIG. 4. Expression of proinflammatory cytokines TNF-α (A) and IL-1β (B) in relationship to the progression of liver fibrosis in chronic hepatitis C patients. Relative mRNA levels for TNF-α (A) and IL-1β (B) genes in 55 biopsy liver samples are plotted according to the disease stage defined by liver fibrosis. Approaches for the determination of the relative mRNA levels are described under *Materials and Methods*. Degrees of statistical significance were analyzed by one-way ANOVA with a post hoc test (Tukey's multiple comparison test). N.S., not significant ($p > 0.05$).

with 4 ng/ml recombinant IL-1β, 50 ng/ml recombinant IL-6, or 0.25 ng/ml recombinant TNF-α at 37°C for 24 h exactly in the same way as HepG2 cells. Our preliminary experiments on *p*-nitrophenol oxidation using human hepatocyte no. 2 showed that IL-1β and TNF-α almost completely suppressed the activity, whereas IL-6 showed only 44% inhibition despite no appreciable change in mRNA expression. Apparently, regulatory mechanisms of CYP2E1 seemed quite different between HepG2 and human primary hepatocytes. Expressed levels of drug transporters, NTCP, OATP-C, and OCT-1, after normalization by GAPDH, were roughly 100-, 1000-, and 10-fold higher in primary hepatocytes than HepG2, respectively. Our preliminary data suggested IL-6 down-regulation by larger than 45% of CYP1A2, CYP3A4, NTCP, OATP-C, and OCT1 in the hepatocytes of the two human individuals. Our present in vitro study using HepG2 and primary hepatocytes may indicate both systems should be used complementarily to clarify mechanisms for cytokine-mediated down-regulation of drug metabolism and disposition genes.

Discussion

There has been little information published on which genes involved in drug metabolism and disposition undergo alteration of their expression during chronic hepatitis C viral infection. Because data

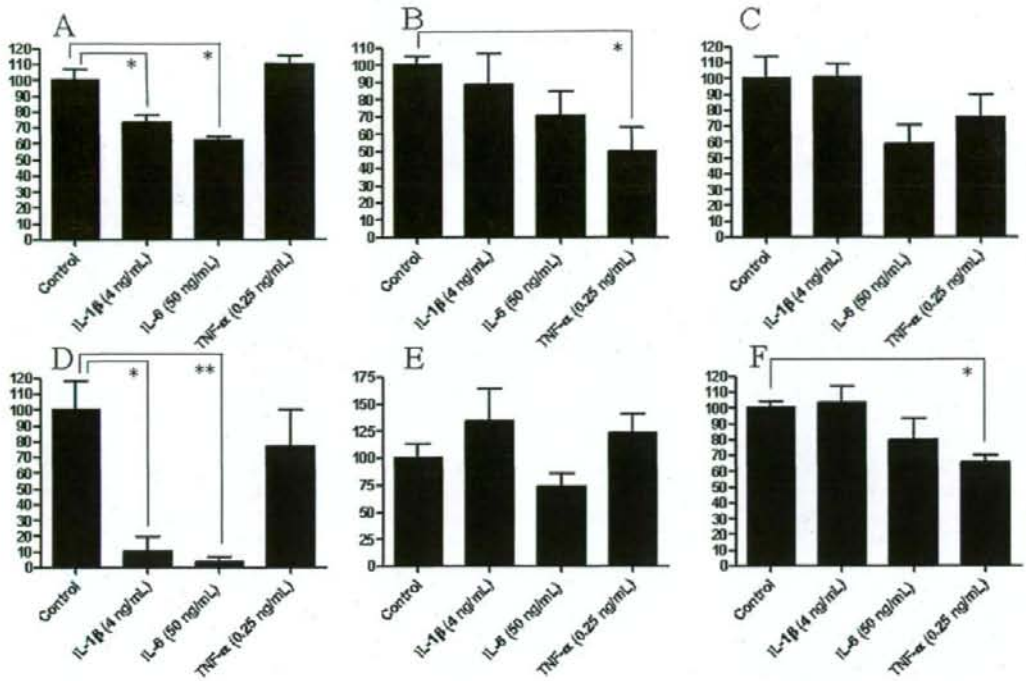

FIG. 5. Expression of CYP1A2 (A), CYP2E1 (B), CYP3A4 (C), NTCP (D), OATP-C (E), and OCT1 (F) mRNA levels in HepG2 cells after 24-h exposure to proinflammatory cytokines IL-1β, IL-6, or TNF-α. HepG2 cells were exposed to IL-1β, IL-6, or TNF-α at 37°C for 24 h as described under *Materials and Methods*. Data are expressed as mean ± S.D. from three separate experiments. Degree of statistical significance of the difference of mRNA levels between control (solvent) and each cytokine-treated group was analyzed by one-way ANOVA with Dunnett post hoc test. Statistical significance is indicated by *and **, which represent $p < 0.05$ and $p < 0.01$, respectively.

have been accumulating on substrate specificities and function for a number of cytochromes P450 and drug transporters, it is valuable to elucidate the changes in gene expression for those cytochromes P450 and transporters for which information is available. We have examined chronic hepatitis C-related changes in the expression of drug metabolism and disposition genes using total RNA extracted from liver biopsy samples from 63 Japanese patients who were diagnosed with chronic hepatitis C at Toranomon Hospital, Tokyo, Japan. The patients recruited in this study exhibited a tendency toward higher values of prothrombin times (INR) and hyaluronic acid levels with HCV-related liver fibrosis progression (Fig. 2).

In agreement with these clinical laboratory observations, a remarkable decrease in CYP1A2, CYP2E1, CYP3A4, NTCP, OATP-C, and OCT1 mRNA levels was observed in relationship to liver fibrosis progression (Fig. 3). Hepatic expressions of CYP1A2, CYP2E1, NTCP, and OCT1 in the initial fibrosis stage (F_1) of hepatitis C infection seemed to be once up-regulated as compared with non-HCV patients according to the statistical analyses throughout non-HCV and F_1 to F_3 HCV patients (Fig. 3). This hypothesis should be evaluated by further studies using liver specimens obtained in one hospital. These mRNA levels overall showed negative correlations with clinical laboratory results of aspartate amino transferase, prothrombin time (INR), and hyaluronic acid (K. Nakai, unpublished data). However, no fibrosis stage-dependent decrease was observed for any of the other genes studied, including CYP2D6 and MDR1 (plots not shown). Only some of the drug metabolism and disposition gene expressions showed fibrosis-stage dependent decrease. During fibrosis progression, fibrotic hepatocytes would be replaced by fibroblasts. This might lead an assumption that a few hepatic genes would not be simultaneously down-regulated. The present study excludes this most trivial explanation on mechanisms of down-regulation of hepatic genes. In conjunction with the inflammatory state of hepatitis C infection, an increase in the TNF-α mRNA level was manifested with the progress of liver fibrosis staging (Fig. 4).

We found a clear relationship between the decrease in hepatic CYP1A2 expression and fibrosis stage progression (Fig. 3A) and inflammation grading (plot not shown) in patients with chronic HCV infection, which is generally consistent with observations by Congiu et al. (2002). CYP1A2, but not CYP4A, decreased at both the mRNA and protein levels during sepsis progression in the rat. Cytochrome P450 blockade by pretreatment with 1-aminobenzotriazole exacerbated the inflammatory response in sepsis (Crawford et al., 2004). These results, together with the finding that CYP1A2 has a protective role against ROS production (Shertzer et al., 2004), indicate that reduction in CYP1A2 expression during HCV infection state might be deleterious. A number of reports in the literature observed that there is a reduction of CYP2E1 expression in chronic HCV infection (Gochee et al., 2003; Asselah et al., 2005; Bièche et al., 2005). The results of this study are consistent with those reports. CYP2E1 has been documented to have a role in ROS generation during exposure of mammalian cells to ethanol, a CYP2E1 substrate/inducer (Navasumrit et al., 2000). Singlet oxygen ($^1O_2$) has been suggested to be involved in CYP2E1 function (Hayashi et al., 2005). Oxidative stress by ethanol has been associated with ethanol-induced and -metabolizing CYP2E1, converting it to more reactive intermediates (Kessova and Cederbaum, 2003). The HCV core protein, in coordination with ethanol, was reported to increase oxidative stress (Wen et al., 2004). The findings using CYP2E1-overexpressing cells have been reviewed